MANITOBA GEOLOGICAL SURVEY
MGS
1928

OF2017-3

OPEN FILE

Preliminary geology of the diamond occurrence at southern Knee Lake, Oxford Lake–Knee Lake greenstone belt, Manitoba (NTS 53L15)

By
S.D. Anderson

Manitoba

Open File OF2017-3

Preliminary geology of the diamond occurrence at southern Knee Lake, Oxford Lake–Knee Lake greenstone belt, Manitoba (NTS 53L15)

by S.D. Anderson

Winnipeg, 2017; reprinted with minor revisions, October 2017

Growth, Enterprise and Trade

Hon. Blaine Pedersen
Minister

Dave Dyson
A/Deputy Minister

Jim Crone
A/Assistant Deputy Minister

Manitoba Geological Survey

Chris Beaumont-Smith
Director

Anderson, S.D. 2017: Preliminary geology of the diamond occurrence at southern Knee Lake, Oxford Lake–Knee Lake greenstone belt, Manitoba (NTS 53L15); Manitoba Growth, Enterprise and Trade, Manitoba Geological Survey, Open File OF2017-3, 27 p.

NTS grid: 53L15

Keywords: alkaline lamprophyre; Archean; chromite; Cr-spinel; Cr-diopside; diamond exploration; Hayes River group; indicator minerals; Knee Lake; lamprophyric volcanism; Manitoba; microdiamonds; Oxford Lake group; Oxford Lake–Knee Lake belt; Oxford–Stull domain; pelletal lapilli; Superior province; unconventional diamondiferous rocks

Published by:

Manitoba Growth, Enterprise and Trade
Manitoba Geological Survey
360–1395 Ellice Avenue
Winnipeg, Manitoba
R3G 3P2 Canada

Telephone: 1-800-223-5215 (General Enquiry)
204-945-6569 (Publication Sales)
Fax: 204-945-8427

E-mail: minesinfo@gov.mb.ca

Website: manitoba.ca/minerals

ISBN No.: 978-0-7711-1586-8

This publication is available to download free of charge at manitoba.ca/minerals

Cover illustration: Outcrop photographs of geochemically primitive, alkaline volcanic sandstone of the ultramafic facies association at southern Knee Lake, showing the sculpted weathered surfaces that characterize outcrops of these rocks (field of view in both photos is approximately 3 m). Sandstone in the upper photograph is massive, whereas in the lower photograph it contains horizontal beds, which in some cases are internally convolute (upper bed), possibly due to dewatering or slumping. The unusual appearance of the outcrop in the lower photograph is due to preferential erosion at the waterline and along vertical joints. These outcrops are located up-section and along strike to the east of the diamondiferous volcanic conglomerate described in this report.

Abstract

In 2016, bedrock mapping and sampling by the Manitoba Geological Survey resulted in the discovery of microdiamonds in shoreline outcrop at southern Knee Lake. The microdiamonds are hosted by polymictic volcanic conglomerate and volcanic sandstone belonging to the Oxford Lake group (ca. 2.72 Ga) of the Oxford Lake–Knee Lake greenstone belt in the northwestern Superior province. Well-preserved primary features indicate deposition as debris and turbidity flows in an alluvial or shallow-marine fan setting, whereas interlayers of lapilli tuff record influxes of primary pyroclastic material. Whole-rock geochemical data indicate primitive bulk compositions (16.7–18.7 wt. % MgO; >500 ppm Cr, Ni) and alkaline affinities (1.2–3.3 wt. % K_2O) for the volcanic sedimentary rocks and lapilli tuff, collectively referred to as the 'ultramafic facies association', and are comparable to alkaline lamprophyre dikes in the Knee Lake area, suggesting an association with lamprophyric volcanism. Diverse clast types in the conglomerate include pyroxenite, gabbro and basalt, presumably derived from the Hayes River group (ca. 2.83 Ga), representing the local basement. Distinctive cored lapilli in the diamondiferous conglomerate are interpreted to represent pelletal lapilli that formed during intensive degassing within a diatreme vent and were subsequently reworked by sedimentary processes. Multiphase ductile deformation fabrics, greenschist-facies metamorphic assemblages (actinolite-chlorite-biotite-epidote), and interstratification with dacitic volcanic rocks dated at 2722 ±3 Ma confirms the Archean emplacement age, placing this diamond occurrence amongst the oldest known on Earth. Indicator minerals in the conglomerate consist of chromite and Cr-spinel, whereas the associated lapilli tuff contains chromite, Cr-diopside, Cr-spinel and diamond-inclusion Cr-spinel, indicative of a mantle-derived magmatic precursor sourced from within the diamond stability field (>140 km depth). Indicator mineral compositions, coupled with the absence of garnet and ilmenite, suggest that the magmatic precursor was not kimberlitic. Microdiamonds (n = 144) obtained from a 15.8 kg sample of the volcanic conglomerate are variable in colour, morphology and degree of resorption, with the largest stone weighing 0.2071 mg (0.00104 ct); a sample of the lapilli tuff did not yield diamonds, whereas lamprophyre dikes at Knee Lake have yet to be assessed for diamonds or indicator minerals.

Unconventional diamond occurrences hosted by lamprophyre dikes, polymict volcaniclastic breccia and conglomerate in the Michipicoten greenstone belt (south-central Superior province) near Wawa, Ontario, provide a useful analog to the occurrence at southern Knee Lake, with implications for exploration. As is the case in the Wawa area, the types and compositions of indicator minerals hosted by the lamprophyric rocks at Knee Lake are distinctly different from the kimberlitic indicator minerals found in surficial sediments; the former are compatible with 'typical' mantle-derived rocks such as komatiite or primitive arc basalt, which are major constituents of greenstone belts in the northwest Superior province. Consequently, any exploration strategy that employs drift prospecting will require careful consideration of not only the complex surficial geology and ice-transport history in the Knee Lake region, but also the potentially diverse and extensive sources of indicator minerals.

TABLE OF CONTENTS

Page

TABLES

FIGURES

APPENDICES

Introduction

In March 2017 the Manitoba Geological Survey (MGS) and a group of independent diamond explorers (the 'Lynx Consortium') announced the discovery of microdiamonds at southern Knee Lake, approximately 200 km southeast of Thompson, Manitoba (Manitoba Government, news release, March 6, 2017). The microdiamonds are hosted by Archean (ca. 2.72 Ga) conglomerates in the central portion of the Oxford Lake–Knee Lake greenstone belt of the western Superior province. The unusual field and geochemical characteristics of these conglomerates had been recognized for more than 50 years. However, it was only through a collaborative partnership between the MGS and the Lynx Consortium that these rocks were sampled, processed and analysed for diamonds and indicator minerals, with one sample (15.8 kg) yielding 144 microdiamonds. This discovery has generated renewed interest in diamond exploration in the Knee Lake area, close to 20 years after the diamond potential was first identified during a regional geochemical sampling program conducted by the MGS. This report provides a preliminary description of the geology of the southern Knee Lake microdiamond occurrence, including aspects of the regional and local geological setting; hostrock lithology, stratigraphy, geochemistry and structure; microdiamond and indicator mineral analytical results; and exploration implications.

Previous work

The earliest geological investigations in the Oxford Lake–Knee Lake belt involved route surveys of the Hayes River (Bell, 1879, 1881; Brock, 1911; McInnes, 1913; Bruce, 1920) and bedrock mapping of Oxford Lake and Knee Lake by the Geological Survey of Canada (Wright, 1926, 1932; Quinn, 1955). Follow-up work by the Manitoba Geological Survey included regional bedrock mapping at 1:31 680 scale (Barry, 1959, 1960, 1964; Gilbert, 1985; Hubregtse, 1985), and thematic studies of alkaline rocks and granitic pegmatite (Hubregtse, 1978; Brooks et al., 1982; Lenton, 1985).

In 1997 and 1998, shoreline exposures on Knee Lake were remapped at 1:20 000 scale by the MGS as part of the Western Superior NATMAP Project, with the objectives of better understanding the volcanic, structural and tectonic evolution of the belt (Syme et al., 1997, 1998, 1999; Lin et al., 1998; Corkery et al., 2000; Lin and Jiang, 2001). Between 1999 and 2001, the MGS also completed a helicopter-supported multimedia geochemical and mineralogical survey (Operation Superior) to assess the mineral resource potential of major greenstone belts in the region, including the Oxford Lake–Knee Lake belt (Fedikow et al., 2000, 2001, 2002a, b). More recently, the Cinder Lake alkaline intrusive complex was investigated by Chakhmouradian et al. (2008), Kressall et al. (2010) and Kressall (2012).

In 2012, the MGS began renewed studies of bedrock and surficial geology in the Oxford Lake–Knee Lake area, with the goal of stimulating exploration activity in the region. Between 2012 and 2016, shoreline outcrops at Oxford Lake and southern and central Knee Lake were remapped at 1:20 000 scale (Anderson et al., 2012a–c, 2013a–d, 2015a, b, 2016; Anderson, 2016a, b). In addition, the regional surficial geology was updated at 1:50 000 scale (Trommelen, 2014a–d) and the glacial history and till composition were examined to provide practical guides for drift prospecting (Trommelen, 2015). Most recently, new analytical data (65 elements) for archival lake sediment samples collected during the National Geochemical Reconnaissance program (1986) were released by the MGS and GSC (McCurdy et al., 2016), and cover the entire Oxford Lake–Knee Lake region.

Exploration history

Exploration activity has been intermittent in the region since the initial discovery of gold in the southern part of Knee Lake in 1918. Early prospecting activity peaked in 1935 and 1936, spurred by underground development of the Knee Lake and Johnston Knee Lake gold mines (Barry, 1964). Since that time the region has been explored at reconnaissance scale, mainly for gold, base metals and diamonds. Concerted exploration for gold took place at western Oxford Lake and southern Knee Lake in the 1980s and for base metals in the Cinder Lake area in the 1990s. As described below, the entire region was explored for kimberlite-hosted diamonds in the late 1990s and early 2000s by a number of major mining companies. However, no economic mineral deposits (or kimberlite) have been identified to date. Mineral occurrences in the region were described by Wright (1926, 1932), Barry (1959, 1960, 1964), Southard (1977) and Richardson and Ostry (1996).

Chronology of work leading to the Knee Lake diamond discovery

The discovery of diamonds at Knee Lake came about incrementally through several decades of geological investigations in the region. Conspicuous layers of bright green chloritic tuff and lapilli tuff along the south shore of Knee Lake were described by Barry (1959; unit 2b) and Gilbert (1985; unit 8h). Whole-rock geochemical analyses reported by Gilbert (1985) indicated primitive bulk compositions (45.5–47.5 wt. % SiO_2; 13–17 wt. % MgO) and alkaline affinities (1.7–3.8 wt. % K_2O). Turbidite bedforms in these layers were interpreted to indicate deposition in a largely subaqueous setting, coeval with alkaline (shoshonite) flows and coarse fragmental rocks of various bulk compositions, collectively representing a submarine volcanic edifice.

Syme et al. (1997) described distinctive layers of ultramafic conglomerate at southern Knee Lake, corresponding to Gilbert's unit 8h and containing pebbles and cobbles of serpentinite, pyroxenite, peridotite, gabbro and basalt in a chloritic sandstone matrix. The ultramafic–mafic clasts were speculated to derive from erosion of a subaerial plutonic massif and associated basalts, perhaps representing oceanic crust (i.e., ophiolite). Unpublished geochemical data from samples collected by these authors confirmed the primitive bulk composition (16.7 wt. % MgO) and alkaline affinity (3.3 wt. % K_2O) of the chloritic sandstone.

Multimedia geochemical and mineralogical surveys of the Knee Lake area by MGS (Operation Superior) subsequently revealed anomalous concentrations of kimberlite indicator minerals (KIMs) in glacial till and beach sand, interpreted to define a dispersal train through central Knee Lake (Fedikow et

al., 2002a). The KIMs include Cr-diopside, G9 and G10 garnet, Mg-ilmenite and Cr-spinel, the latter including a single grain of diamond inclusion type. Follow-up exploration by a number of companies between 1999 and 2004 utilizing high-resolution geophysical surveys, heavy mineral sampling of surficial materials and percussion drilling of coincident geophysical and geochemical anomalies apparently failed to identify a bedrock source for the KIMs (Syme et al., 2004); there is no evidence that the diamondiferous rocks described herein were evaluated for their diamond potential during these exploration programs.

A detailed re-examination of the outcrops of ultramafic conglomerate at southern Knee Lake in 2008 by R. Syme and S. Anderson (MGS) revealed spherical, cored clasts that are superficially similar in appearance to pelletal lapilli found in primary or reworked volcaniclastic deposits associated with diatreme pipes. Whole rock geochemical data for clasts in the conglomerate indicated variable bulk compositions (46–54 wt. % SiO_2; 6.3–14.8 wt. % MgO; 0.3–2.3 wt. % K_2O; Syme and Anderson, 2008, unpublished data). Interestingly, the composition of the matrix was found to be more primitive and alkaline (16.8 wt. % MgO; 3.0 wt. % K_2O) than any of the clasts, suggesting derivation from a different source.

Also in 2008, prospector R. Day collected a sample of polymictic conglomerate from a shoreline outcrop (Archean bedrock) in northern Knee Lake. An 8 kg split of this sample was processed by caustic fusion at Geoanalytical Laboratories Diamond Services of the Saskatchewan Research Council (SRC) and yielded one microdiamond—a colourless, transparent, resorbed, octahedron weighing 0.01 mg—possibly representing the first discovery of diamond in bedrock in Manitoba. In 2012, at the direction of M. Fedikow (formerly MGS), the remaining split of the original sample collected by R. Day was processed by SRC for caustic fusion analysis (14.3 kg sample) and heavy mineral separation (17.8 kg sample). This analysis failed to yield additional diamonds, but did yield 10 indicator mineral grains, including olivine (5), Mg-ilmenite (4) and Cr-diopside (1).

In 2015, southern Knee Lake was remapped by MGS. The primitive alkaline rocks were described to consist of two facies: lapilli tuff and tuff of primary pyroclastic derivation and reworked volcanic material, consisting of conglomerate, sandstone and mudstone, collectively assigned to the 'ultramafic facies association' of Anderson et al. (2015a, b; units 11a and 11b). The primitive chemistry (17.6 wt. % MgO; 1200 ppm Cr; 1020 ppm Ni) and strongly alkaline affinity (3.1 wt. % K_2O) were noted to be similar to diamondiferous lamprophyre and associated polymict volcaniclastic breccia (e.g., Lefebvre et al., 2005) in the Michipicoten greenstone belt near Wawa, Ontario, which was taken to indicate that these rocks may similarly derive from lamprophyric volcanism (Anderson et al., 2015b), with the implication that they may also be diamondiferous.

In January 2016, M. Fedikow presented the proprietary microdiamond and indicator mineral data from the conglomerate outcrop at northern Knee Lake to S. Anderson. At the request of M. Fedikow, this locality was examined by S. Anderson during continued bedrock mapping at Knee Lake in July 2016; it was found to consist of fluvial polymictic conglomerate with abundant well-rounded tonalite cobbles and minor interbeds of feldspathic greywacke, crosscut in one location by a 40 cm thick diabase dike. On behalf of M. Fedikow, a sample of pebbly greywacke weighing 52 kg was collected from this outcrop for the purpose of confirming the original analytical results. Bulk samples (each weighing ~32 kg) were also collected from two outcrops of the ultramafic facies association at southern Knee Lake, at sites selected by S. Anderson on the basis of similarities (Anderson et al., 2015b) to diamondiferous volcaniclastic rocks near Wawa, Ontario; these primitive alkaline rocks were thought to be good candidates to host diamonds, with no record of having been processed for heavy minerals or diamonds previously.

The three samples collected in 2016 by the MGS were provided to M. Fedikow under a Memorandum of Understanding, which stipulated that the samples were to be submitted to a certified laboratory for caustic fusion microdiamond recovery, heavy mineral separation and indicator mineral chemistry, with all analytical costs to be borne by M. Fedikow and all resulting data provided to MGS for the purpose of informing continued mapping and research in the Knee Lake belt. Costs were subsequently shared among Mount Morgan Resources Ltd. (M. Fedikow), Polaris Capital Ltd. (R. Day), Indicator Explorations Ltd. (J. Lee) and H. Westdal (independent prospector), collectively forming the 'Lynx Consortium'.

In November 2016, caustic fusion and heavy mineral processing at the Geoanalytical Laboratories of the Saskatchewan Research Council yielded the following results, with 'LX' and 'KL' denoting sample splits processed for microdiamonds and indicator minerals, respectively.

1) Polymictic tonalite-clast conglomerate, northern Knee Lake (R. Day locality): 0 microdiamonds (sample LX-1; 20.3 kg); 19 indicator mineral grains (sample KL-1; 5.5 kg), including garnet (G9, G11, G10D, G3 and G0; classification scheme of Grütter et al., 2004), ilmenite, chromite, olivine and rutile.
2) Volcanic conglomerate with pelletal lapilli, southern Knee Lake (S. Anderson locality): 144 microdiamonds (sample LX-2; 15.8 kg); 52 indicator mineral grains (sample KL-2; 6.4 kg), including chromite, Cr-spinel and tourmaline.
3) Lapilli tuff, southern Knee Lake (S. Anderson locality): 0 microdiamonds (sample LX-3; 16.3 kg); 70 indicator mineral grains (sample KL-3; 5.4 kg), including chromite, Cr-diopside, Cr-spinel, diamond-inclusion Cr-spinel, olivine and amphibole.

Thus, each of the three localities is distinctly different not only in field characteristics but also in microdiamond and indicator mineral content. The locality at northern Knee Lake consists of an isolated outcrop for which little other information or geological context exists, and processing of two larger samples from this site has failed to reproduce the original microdiamond results. In contrast, considerable information is available for the two localities at southern Knee Lake and follow-up sampling has confirmed the presence of diamonds (Altius Minerals Corporation, press release, September 25, 2017). Consequently, this preliminary report is focused on documenting the geology of the southern Knee Lake occurrence, in order to provide constraints for on-going exploration.

Regional setting

The Oxford Lake–Knee Lake greenstone belt (Figure 1) is situated in the western portion of the Oxford–Stull domain of the western Superior province, approximately 110 km inboard from the craton margin. This domain consists of ca. 2.9–2.7 Ga volcanic and plutonic rocks with mostly juvenile isotopic signatures and Nd model ages less than 3.0 Ga, thought to represent a tectonic collage of oceanic and continental-margin affinity (Skulski et al., 2000; Percival et al., 2006; Stott et al., 2010). It is bounded to the north across the North Kenyon fault by the Hudson Bay terrane of Stott et al. (2010), which is characterized by gneissic rocks with older Nd model ages (3.6–2.9 Ga) and inherited zircon ages up to 3.6 Ga, indicative of a relatively ancient continental affinity (Skulski et al., 2000; Percival et al., 2006). To the south, the Stull-Wunnummin fault separates the Oxford–Stull domain from other tectonic components of the North Caribou terrane, which contains widespread isotopic evidence for ca. 3.0 Ga crust and is interpreted to represent the protocratonic nucleus of the western Superior province (Percival et al., 2006; Stott et al., 2010). These fault-bounded crustal blocks are thought to have been juxtaposed by ca. 2.72 Ga collision of the Hudson Bay and North Caribou terranes during amalgamation of the western Superior province (Skulski et al., 2000; Lin et al., 2006; Percival et al., 2006).

The Oxford Lake–Knee Lake greenstone belt

The Oxford Lake–Knee Lake belt is the largest and most contiguous greenstone belt in the Oxford–Stull domain (Figure 1). It has historically been subdivided into two principal stratigraphic units: the older Hayes River group (HRG) and younger Oxford Lake group (OLG). The HRG consists of pillowed basalt flows and subvolcanic gabbro sills, with minor intermediate–felsic volcanic, volcaniclastic and turbiditic sedimentary rocks, and iron formation (Gilbert, 1985; Hubregtse, 1985; Syme et al. 1997, 1998; Anderson et al., 2013d, 2015b; Anderson, 2016b). Geochemical characteristics indicate significant crustal input, similar to modern volcanic arc and back-arc basin settings, although a small subset of samples have strongly depleted signatures similar to modern mid-ocean ridge basalt (Syme et al., 1999). The type sections of the HRG at central Oxford Lake and southern Knee Lake approach 10 km in thickness and define homoclinal panels (Anderson et al., 2013d, 2015b), representing either a primary stratigraphic succession (Gilbert, 1985; Hubregtse, 1985) or a tectonic collage (Syme et al., 1999). U-Pb zircon dating of felsic volcanic rocks indicate that volcanism spanned roughly 10 m.y., between ca. 2835 and 2825 Ma (Corkery et al., 2000; Syme et al., 2008, unpublished data; Anderson et al., 2012, 2013, unpublished data). The base of the HRG is everywhere defined by granitoid rocks across

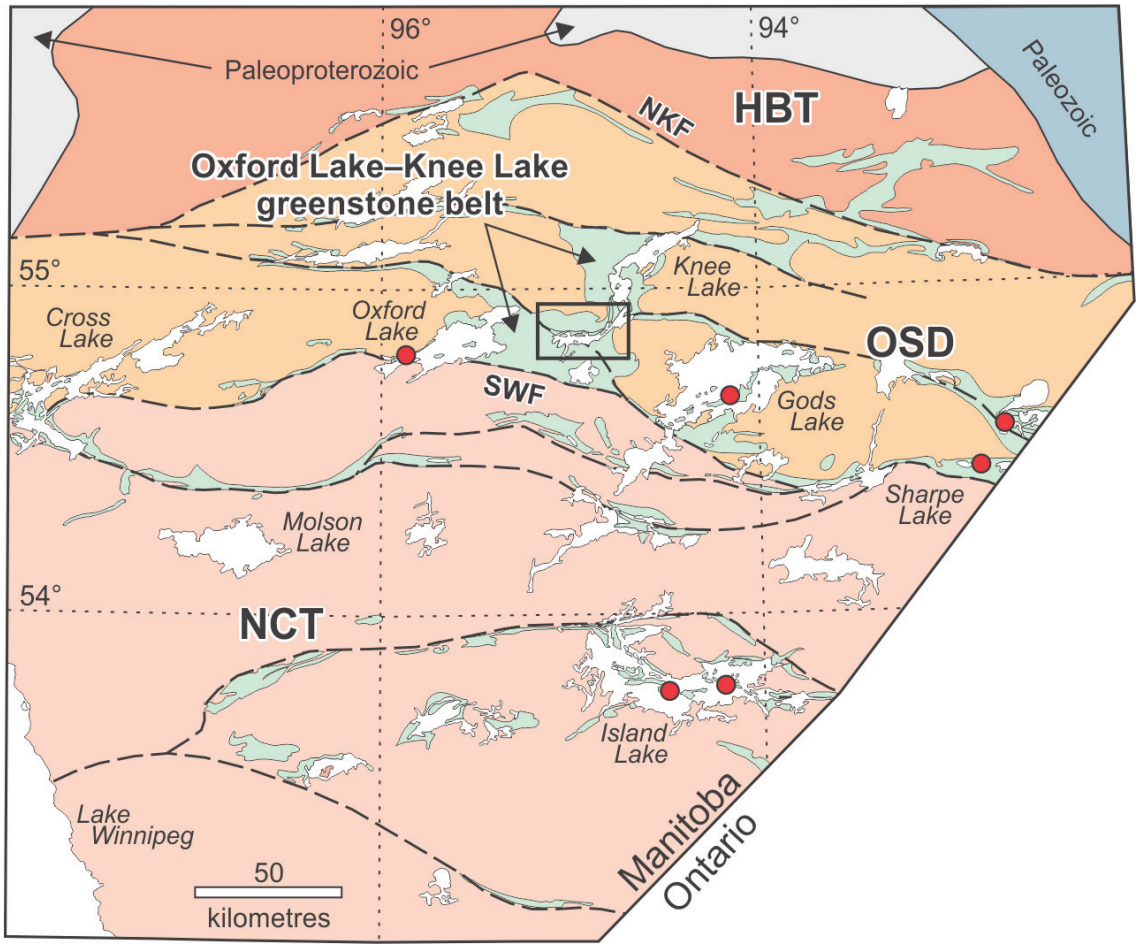

Figure 1: *Regional geological setting of the Oxford Lake–Knee Lake greenstone belt in the northwestern Superior province (terminology after Stott et al., 2010). Significant gold deposits are indicated by red circles. Abbreviations: HBT, Hudson Bay terrane; NCT, North Caribou terrane; NKF, North Kenyon fault; OSD, Oxford–Stull domain; SWF, Stull-Wunnummin fault. Location of Figure 2 is outlined.*

tectonic or intrusive contacts, whereas the top is defined by faults or an unconformity.

The OLG overlies the HRG and consists of marine volcanic, volcaniclastic and derived sedimentary rocks, the latter being the most extensive. The volcanic rocks are calcalkaline to alkaline (shoshonitic), range in composition from basalt to rhyolite and include coherent flows and associated coarse fragmental and epiclastic deposits (Hubregtse, 1978, 1985; Brooks et al., 1982; Gilbert, 1985; Syme et al., 1997; Anderson et al., 2013d). The thickest and most continuous sections are found at eastern Oxford Lake and southern Knee Lake, where they have a minimum stratigraphic thickness of 2 km. Associated sedimentary rocks include thick successions of submarine-fan conglomerate and sandstone of volcanic derivation, with minor iron formation and basalt–andesite flows. Hypabyssal intrusions of shoshonitic affinity in the underlying HRG (Anderson et al., 2015b) confirm it as the local basement during deposition of the OLG. U-Pb zircon dating of felsic volcaniclastic rocks at Oxford Lake and Knee Lake indicate that volcanism spanned roughly 20 m.y., between ca. 2725 and 2705 Ma (Corkery et al., 2000; Lin et al., 2006).

Sandstone and polymictic conglomerate overlie the HRG and OLG, and contain large-scale trough crossbeds, channel-fills and pebble–cobble lag deposits characteristic of fluvial-alluvial sequences. These rocks were previously included in the OLG, but new mapping and detailed structural analysis at central Knee Lake demonstrates that these rocks are bounded at the base by an angular unconformity and at the top by faults, and are thus broadly synorogenic (Anderson, 2016b). Abundant granitoid and vein-quartz clasts in the conglomerates indicate regional uplift and erosion, and the relative paucity of crosscutting intrusions indicates deposition during the waning stages of regional magmatism. U-Pb dating of detrital zircons indicates maximum depositional ages of ca. 2710 Ma (Corkery et al., 2000; Syme et al., 2008, unpublished data; Anderson et al., 2012, unpublished data).

The Oxford Lake–Knee Lake belt is everywhere bounded by granitoid intrusions that include tonalite to granodiorite gneiss, tonalite, quartz diorite, granodiorite, granite and syenite. Most of these intrusions were traditionally included in the 'Bayly Lake complex', which was interpreted to post-date the HRG and pre-date the OLG (Gilbert, 1985; Hubregtse, 1985). However, U-Pb zircon geochronological data for the region indicate that granitoid magmatism spanned at least 200 million years, in four broad pulses: pre-HRG (ca. 2880–2845 Ma), post-HRG–pre-OLG (ca. 2815–2780 Ma), syn-OLG (ca. 2735–2705 Ma) and post-OLG (ca. 2670 Ma) (e.g., Skulski et al., 2000; Lin et al., 2006; Chakhmouradian et al., 2008; Kressall et al., 2010; Anderson et al., 2012, unpublished data). Much older zircons (>2.9 Ga) have been identified as inherited grains in tonalite gneiss and as detrital grains in synorogenic sandstone (Corkery et al., 2000; Skulski et al., 2000; Lin et al., 2006), indicating that older crust may exist in the region.

Geology of southern Knee Lake

Each of the principal components of the Oxford Lake–Knee Lake belt is exposed in shoreline outcrop at southern Knee Lake (Figure 2). The HRG and OLG wrap broadly around the margins of granitoid plutons. Internal map patterns are disrupted by shear zones and faults; those of the OLG are further complicated by isoclinal folds. In the west, a subparallel series of arcuate shear zones generally trends toward the northwest and includes two first-order strands: the Long Island shear zone (LISZ) on the north and the Taskipochikay Island shear zone (TISZ) on the south (these structures roughly correspond to the Southern Knee Lake shear zone of Lin et al., 1998). The LISZ separates HRG on the north from OLG on the south, whereas the TISZ coincides with a southward transition from greenschist to amphibolite-facies metamorphism in the OLG. In the east, northeast-trending shear zones separate panels of HRG basalt and a younger panel of turbiditic sandstones. The most easterly shear zone in this arm of the lake marks an abrupt eastward change from greenschist to amphibolite-facies metamorphism in the HRG.

Hayes River group

The HRG is exposed along the northern and eastern shorelines of southern Knee Lake. Pillowed and massive flows of basalt and basaltic andesite dominate and include aphyric, plagioclase-phyric and variolitic units, with minor flow breccia, bedded hyaloclastite and iron formation. Younging directions are consistently toward the south or southeast. A fault-disrupted section of felsic volcanic, volcaniclastic and epiclastic rocks up to 1.5 km in thickness is exposed along the northern shoreline, most notably in Pain Killer Bay (Figure 2). Coherent and fragmental feldspar±quartz-phyric rhyolite (2827 +5/-4 Ma; Corkery et al., 2000) in this unit is intercalated with breccia, tuff breccia and lapilli tuff, and associated volcanic conglomerate, sandstone, mudstone and iron formation. Felsic volcanic rocks containing volcanogenic massive sulphide also occur further down-section in the area southeast of Cinder Lake (Gilbert, 1985; Assessment File 94730, Manitoba Growth, Enterprise and Trade, Winnipeg). Layered subvolcanic ultramafic–mafic sills in the HRG section (Figure 2) are commonly differentiated from peridotite or pyroxenite at the base to leucogabbro or quartz diorite at the top; discordant magnetic features (Assessment File 94884) and coincident drill intercepts of peridotite (Assessment File 91191) further down section are interpreted to represent feeder dikes. Hypabyssal porphyry intrusions of intermediate–felsic composition are abundant in the area of Pain Killer Bay and include a distinct phase of K-feldspar megacrystic porphyry that may represent a hypabyssal phase of the Cinder Lake alkaline intrusive complex, which intrudes the HRG further down-section (see below).

Intrusive rocks

The HRG at southern Knee Lake is intruded by the Bayly Lake and Whitemud Lake plutons, and the Cinder Lake alkaline intrusive complex (Figure 2), as well as minor dikes of mafic to intermediate composition. The absolute ages of the plutons are unknown; as described below, the Cinder Lake alkaline intrusive complex appears to record a protracted emplacement history.

The Bayly Lake pluton defines the eastern margin of the belt and intrudes amphibolite-facies aphyric basalt flows of the HRG. It includes porphyritic granite and granodiorite, the

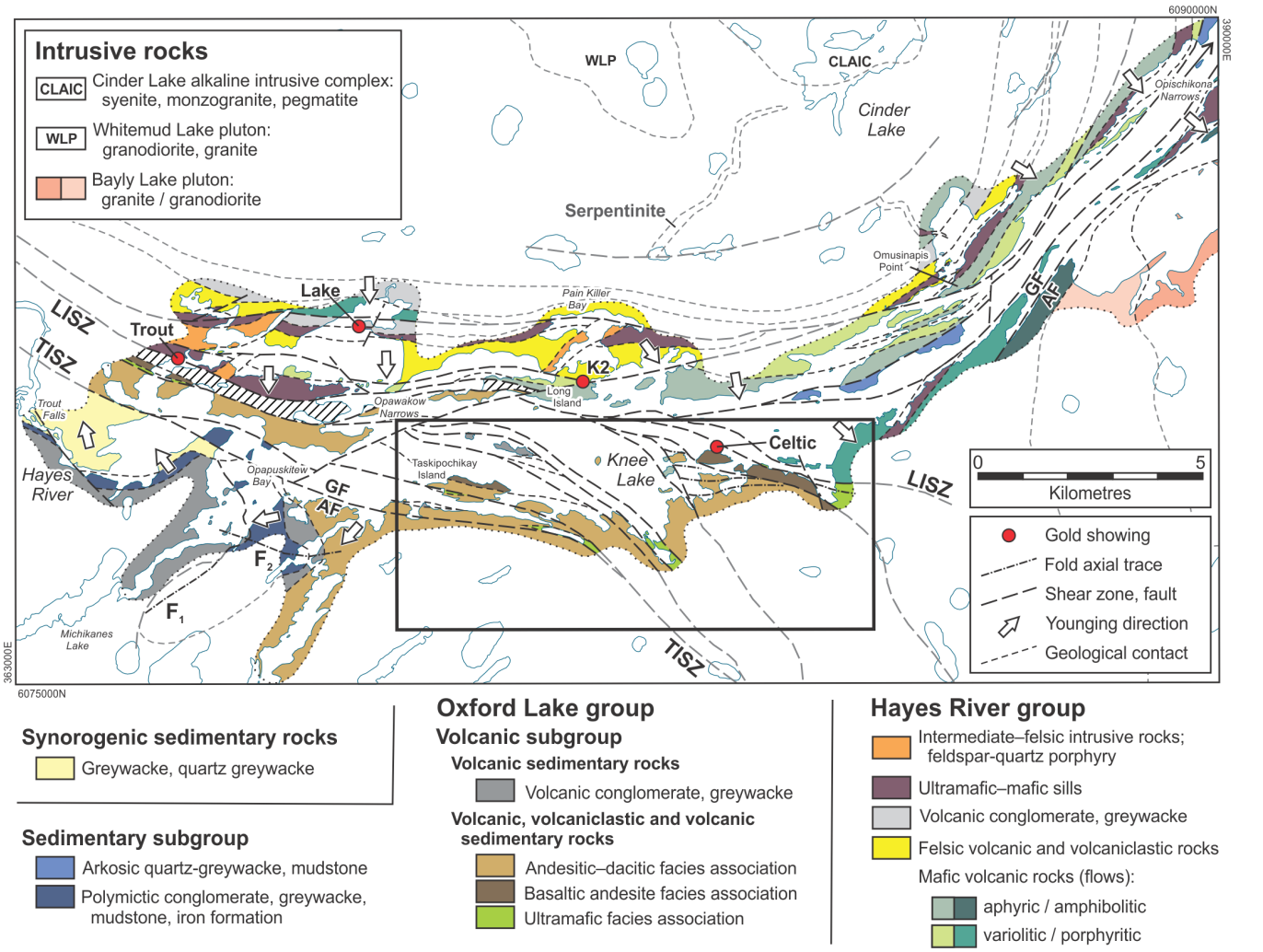

Figure 2: *Simplified geology of the southern Knee Lake area (after PMAP2015-1; Anderson et al., 2015a), including named gold showings and geographic features. Geology outside the mapping limit is simplified from Gilbert (1985) and high-resolution aeromagnetic data. Hachure pattern indicates undivided tectonite. Abbreviations: AF and GF indicate structural boundaries between amphibolite facies and greenschist facies rocks; LISZ, Long Island shear zone; TISZ, Taskipochikay Island shear zone. Location of Figure 3 is outlined. Dotted line indicates 2015 mapping limit.*

contact relationships of which are uncertain. The granodiorite contains minor inclusions of gabbro and amphibolite and is generally weakly foliated, whereas the granite tends to be moderately or strongly foliated. The Whitemud Lake pluton consists mostly of granodiorite, with minor granite and porphyritic granite (Gilbert, 1985). It is interpreted to underlie the area west of Cinder Lake based on the homogeneous and subdued magnetic signature in this area, which is comparable to, and continuous with, that of the pluton interior farther north.

The Cinder Lake alkaline intrusive complex, located just west of central Knee Lake has recently been studied in detail (Chakhmouradian et al., 2008; Kressall et al., 2010; Kressall, 2012). High-resolution aeromagnetic data (Assessment File 94884) suggest that the complex is elliptical, concentrically zoned and has a maximum diameter of 10 km. It intrudes the HRG and the margin of the Whitemud Lake pluton. The only exposures are along the southeastern rim of the complex at Cinder Lake and consist of fine-grained syenite (cancrinite-nepheline syenite, vishnevite syenite and porphyritic cancrinite syenite), alkali-feldspar syenitic pegmatite and monzogranite. Uranium-lead zircon ages of 2723 ±10 Ma and 2705 ±2 Ma from vishnevite syenite, and 2721 ±16 Ma from monzogranite (Chakhmouradian et al., 2008; Kressall et al., 2010), indicate a complex emplacement history, which was broadly coeval with alkaline volcanism in the OLG (ca. 2725–2705 Ma; Corkery et al., 2000; Lin et al., 2006). Carbonate dikes discovered east of Cinder Lake (Anderson, 2016a, b) have been identified as calcite carbonatite on the basis of mineralogical, geochemical and isotopic evidence (Donak, 2016), but their relationship to the Cinder Lake alkaline intrusive complex remains unknown. Carbonatite dikes are also found at Oxford Lake (Anderson et al., 2012c; Reimer, 2014), suggesting such dikes may be regionally extensive.

Oxford Lake group

The OLG underlies the southern and western portions of southern Knee Lake, and defines a series of monoclinal to tightly folded, fault-bounded structural panels. Following the terminology of previous workers (Gilbert, 1985; Syme et al., 1997; Anderson et al., 2015a, b), the OLG is divided into the

'volcanic subgroup' consisting mostly of volcanic-derived sedimentary rocks, with associated volcanic and volcaniclastic rocks, and the 'sedimentary subgroup' consisting of sedimentary rocks that show evidence of mixed provenance, including clasts of plutonic origin. Fluvial-alluvial sandstone exposed along the Hayes River upstream to Trout Falls was previously included in the sedimentary subgroup of the OLG (Syme et al., 1997; Anderson et al., 2015a, b). However, recent mapping indicates that these rocks are younger (Anderson, 2016b) and they are described below as 'synorogenic sedimentary rocks'.

Volcanic subgroup

The volcanic subgroup was subdivided by Anderson et al. (2015a, b) to include three volcanic 'facies associations': ultramafic (lamprophyric affinity); basaltic andesite (shoshonitic affinity); and andesitic–dacitic (calcalkalic affinity). Each facies association is dominated by volcanic conglomerate and coarse sandstone interpreted as debris and grain flow deposits in channelized subaqueous fans sourced from proximal subaerial or shallow-marine volcanoes (Syme et al., 1997; Anderson et al., 2015b). Local stratigraphic interlayering indicates that the lamprophyric, shoshonitic and calcalkalic volcanism was broadly coeval, perhaps within a volcanic field composed of multiple eruptive centres. Ongoing bedrock mapping, geochemistry and geochronology are focused on resolving the stratigraphic and petrogenetic relationships of these distinct volcanic facies associations.

Ultramafic facies association

The ultramafic facies association contains some of the most distinctive rocks in the entire Oxford Lake–Knee Lake belt, due in part to their chlorite-actinolite mineralogy, and resulting bright olive-green and smoothly sculpted weathered surfaces; these rocks have also since proven to be diamondiferous, as described in detail below. This facies association includes lapilli tuff and tuff, and volcanic conglomerate, sandstone and mudstone (Anderson et al., 2015a, b). It is exposed in several locations, mostly between the LISZ and TISZ, and often displays excellent preservation of primary features, despite coinciding with zones of intense ductile strain (Figure 2). Whole-rock geochemical data indicate primitive bulk compositions and alkaline affinities (Anderson, 2016a), which together with the unusual field characteristics are the distinguishing features of this unit.

Basaltic andesite facies association

The basaltic andesite facies association also contains very distinctive rocks, only observed between the LISZ and TISZ. The best exposures are found on Taskipochikay Island and the small islands to the north, but small exposures also occur at the western end of Knee Lake, and on islands and shoreline in the southeastern corner of the lake. This facies association consists of coherent (pillowed or massive) and fragmental flows of shoshonitic basalt, basaltic andesite and andesite (Anderson, 2016a), and derived volcanic conglomerate, sandstone and mudstone. The shoshonite is abundantly and coarsely plagioclase-phyric (20–50%; 0.5–1.5 cm), with a dark grey biotitic groundmass; some varieties also include pyroxene phenocrysts. Associated volcanic sedimentary rocks contain shoshonite clasts and coarse plagioclase crystals in a biotitic matrix.

Andesitic–dacitic facies association

The andesitic–dacitic facies association is much more widespread at southern Knee Lake: it underlies most of the area between the LISZ and TISZ, and represents the dominant unit south of the TISZ, where it includes thick successions of volcaniclastic material. This facies association includes coherent flows of calcalkalic andesite–dacite, associated breccia, tuff breccia, lapilli tuff and crystal tuff (2722 ±3 Ma; Corkery et al., 2000), and derived volcanic conglomerate, sandstone and mudstone. The andesite–dacite flows contain phenocrysts of plagioclase (<30%; <8 mm) and minor quartz (<5%; <3 mm) in a light grey to green, aphanitic groundmass. Associated epiclastic rocks contain abundant plagioclase crystals (1–3 mm) in a light green-grey, variably biotitic matrix.

Sedimentary subgroup

The sedimentary subgroup of the OLG is found south of the TISZ, where polymictic conglomerate, feldspathic greywacke, mudstone, iron formation and chert define macroscopic refolded isoclinal folds (Anderson et al., 2015a, b). Unlike superficially similar rocks in the volcanic subgroup, the conglomerate beds generally contain rounded tonalite, granodiorite, gabbro and rare vein-quartz clasts. Turbidite bedforms coupled with local iron formation and chert indicate a periodically quiescent submarine-fan depositional setting. Arkosic quartz-greywacke (<2713 Ma; Syme et al., 2008, unpublished data) exposed in the northeast arm of southern Knee Lake forms a fault panel bounded on either side by older basaltic rocks of the HRG. This greywacke weathers a distinctive reddish-pink to brown and contains abundant pebbles and granules of quartz and feldspar, with well developed turbidite bedforms.

Synorogenic sedimentary rocks

Greywacke and quartz greywacke (<2709 +9/-8 Ma; Corkery et al., 2000) exposed along the Hayes River upstream to Trout Falls define a homoclinal panel that ranges up to 800 m in thickness and is bounded to the north by the TISZ (Figure 2). Ubiquitous trough crossbeds indicate a fluvial depositional setting and consistently young to the north. Although previously included in the sedimentary subgroup of the OLG (Syme et al., 1997; Anderson et al., 2015a, b), recent mapping indicates that these rocks are probably equivalent to synorogenic sedimentary rocks at central Knee Lake (Anderson, 2016b), which likewise have a maximum depositional age of ca. 2710 Ma (Syme et al., 2008, unpublished data) and overlie the OLG and HRG unconformably.

Lamprophyre dikes

Lamprophyre dikes are a common, but volumetrically minor, rock type at southern and central Knee Lake, where they intrude the HRG, Bayly Lake pluton, OLG and synorogenic sedimentary rocks. Several compositional types are apparent (Anderson, 2016a), perhaps indicating more than one phase of emplacement. These dikes weather dark green to emerald green

and typically contain 5–20% dark brown or black phlogopite phenocrysts up to 2.5 cm in size in a groundmass composed mostly of fine-grained actinolite and chlorite. The dikes range up to 5 m in thickness and are characterized by sharp planar contacts and thick (3–5 cm) chilled margins; some dikes are flow banded or contain exotic granitoid xenoliths. As described below, the major and trace element geochemistry of some dikes indicate a possible genetic association to diamondiferous rocks of the ultramafic facies association, which would require at least two stages of lamprophyric magmatism (ca. 2.72 Ga and <2.7 Ga) based on field relationships and available U-Pb zircon ages. However, none of the lamprophyre dikes have been directly dated, or processed for diamonds and indicator minerals.

Geology of the sample localities

The thickest, most extensive and best-preserved sections of the ultramafic facies association (UFA) are found in two small bays along the southeastern shore of southern Knee Lake. These locations are referred to informally as the 'eastern bay' and 'western bay' (Figure 3), and one sample from each was collected for microdiamond and indicator mineral processing. Sample LX/KL-2 was collected from volcanic conglomerate in the eastern bay, whereas sample LX/KL-3 was collected from lapilli tuff in the western bay (Figure 3). As noted previously, sample LX/KL-1 was collected from an isolated outcrop of polymictic tonalite-clast conglomerate in northern Knee Lake for which little information exists, and is not discussed further here.

The stratigraphic sections in both the eastern and western bays are disrupted by ductile shear zones and macroscopic tight to isoclinal folds, the latter indicated by reversals in younging directions and local mesoscopic fold closures. Coupled with significant gaps in exposure, the internal stratigraphy of these sections remains poorly understood. Both show commonalities in terms of rock types, sedimentary structures and the overall arrangement of map units, and are described together below. At both locations, the UFA appears to define an overall fining-upward sequence, with a lower section that contains coarse volcanic conglomerate and an upper section that consists mostly of volcanic sandstone. The UFA in the western bay contains coarser conglomerates and beds interpreted to be of primary pyroclastic derivation, consistent with a more proximal facies; these rocks are also intruded by pyroxenite and gabbro sills. The sections exposed in the eastern and western bays may represent parts of a single basin that was disrupted and repeated by folding or faulting or, alternatively, may represent entirely separate basins.

The UFA in the western bay has an apparent thickness of about 250 m, whereas in the eastern bay the apparent thickness varies from approximately 100 to more than 500 m. True stratigraphic thicknesses are unknown due to structural complexities, but are conservatively estimated to be about 75 m in both locations. Detailed aeromagnetic data (Assessment File 94884) indicate that these rocks may extend for several kilometres along strike to the west-northwest under Knee Lake and inland to the southeast under a mostly continuous drift cover.

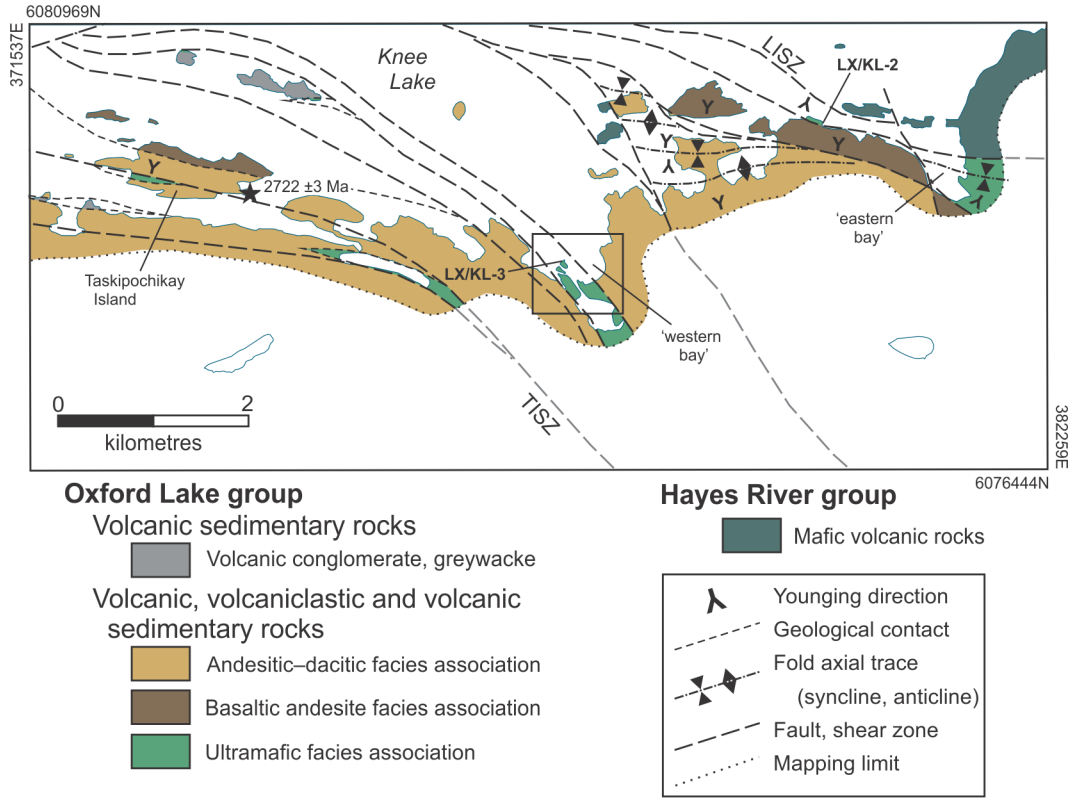

Figure 3: *Simplified geology of southeastern Knee Lake showing occurrences of the ultramafic facies association (UFA), and the locations of the western and eastern bays (type localities for the UFA), and samples LX/KL-2 and LX/KL-3. Location of Figure 4 is outlined.*

In the western bay, the UFA is bounded by rocks assigned to the andesitic–dacitic facies association, which here consists of plagioclase (±quartz, hornblende)-phyric flows and volcaniclastic rocks (Figure 4). Massive crystal tuff is extensive west of the bay; it contains scattered lithic clasts but is otherwise homogeneous, with blocky plagioclase (20–30%; <8 mm) and quartz (2–3%; <4 mm) phenocrysts (Figure 5a). Interbeds of lapilli tuff, tuff breccia and volcanic conglomerate, consisting mostly of porphyritic dacite (Figure 5b), become more abundant toward the east and are interstratified with the UFA indicating a primary stratigraphic relationship (Figure 4). This contact has been disrupted by high strain zones, which are manifest by penetrative S-L shape fabrics. The northeast contact of the UFA is not exposed; it may be primary, perhaps on the opposite limb of a macroscopic fold, or entirely tectonic. Dacitic lapilli tuff of the andesitic–dacitic facies association along strike to the west at Taskipochikay Island (Figure 3) has been dated at 2722 ±3 Ma (Corkery et al., 2000), which is thus interpreted to closely approximate the age of the UFA in the western bay.

In the eastern bay, the UFA is bounded to the southwest by rocks of the basaltic andesite facies association, and to the northeast, across the Long Island shear zone, by mafic flows and sills of the HRG. Neither contact is exposed, but both are presumed to be tectonic on the basis of structural criteria. The basaltic andesite facies association is particularly well exposed along a north-south trending segment of shoreline at the western entrance to the bay and includes a shoshonite flow or cryptoflow (Figure 6a) and a massive, unsorted, clast-supported conglomerate that contains very large (up to several meters) blocks of sandstone and gabbro (Figure 6b), interpreted to represent a proximal debris flow or 'slump deposit' (Syme et al., 1997). Younging criteria indicate a back-to-back structural relationship with the UFA.

Ultramafic facies association – lower sections

The lower sections of the UFA contain coarse, polymictic, volcanic conglomerate, which forms poorly sorted to unsorted beds that range up to several metres in thickness and are interbedded with similarly thick beds of pebbly sandstone. Coarser beds (cobble–boulder; Figure 7a, b) are typically clast supported and massive to normally graded, whereas finer beds (pebble–cobble; Figure 7c, d) are matrix supported and often show well-developed size grading. Basal contacts are typically sharp whereas upper contacts are more diffuse, with the conglomerate grading upward into sandstone. Many beds are deeply scoured at the base, with prominent lag deposits. The clast populations have variable shapes (angular to well rounded) and include a wide variety of volcanic and plutonic material of ultramafic, mafic and intermediate composition, including clasts of pyroxenite, gabbro, basalt and resedimented material. The latter includes abundant intra-formational volcanic conglomerate, sandstone and mudstone clasts (Figure 7a). Some clasts of basaltic composition contain conspicuous phenocrysts of pyroxene. The well-rounded clasts indicate subaerial transport, whereas the intraformational clasts indicate a local provenance for at least some of this detritus. The matrix consists of green, pebbly, medium to coarse-grained chlorite-actinolite sandstone that locally contains large (up to 7 mm) crystals of phlogopite. As described below, whole-rock geochemical data indicate the primitive composition and alkaline affinity of this sandstone. The diamondiferous sample LX/KL-2 was collected from a pebble–cobble conglomerate bed in the eastern bay (Figure 3), from an outcrop that contains several such beds, characterized by scoured basal contacts and continuous normal size-grading upward into medium or coarse-grained pebbly sandstone (Figure 8).

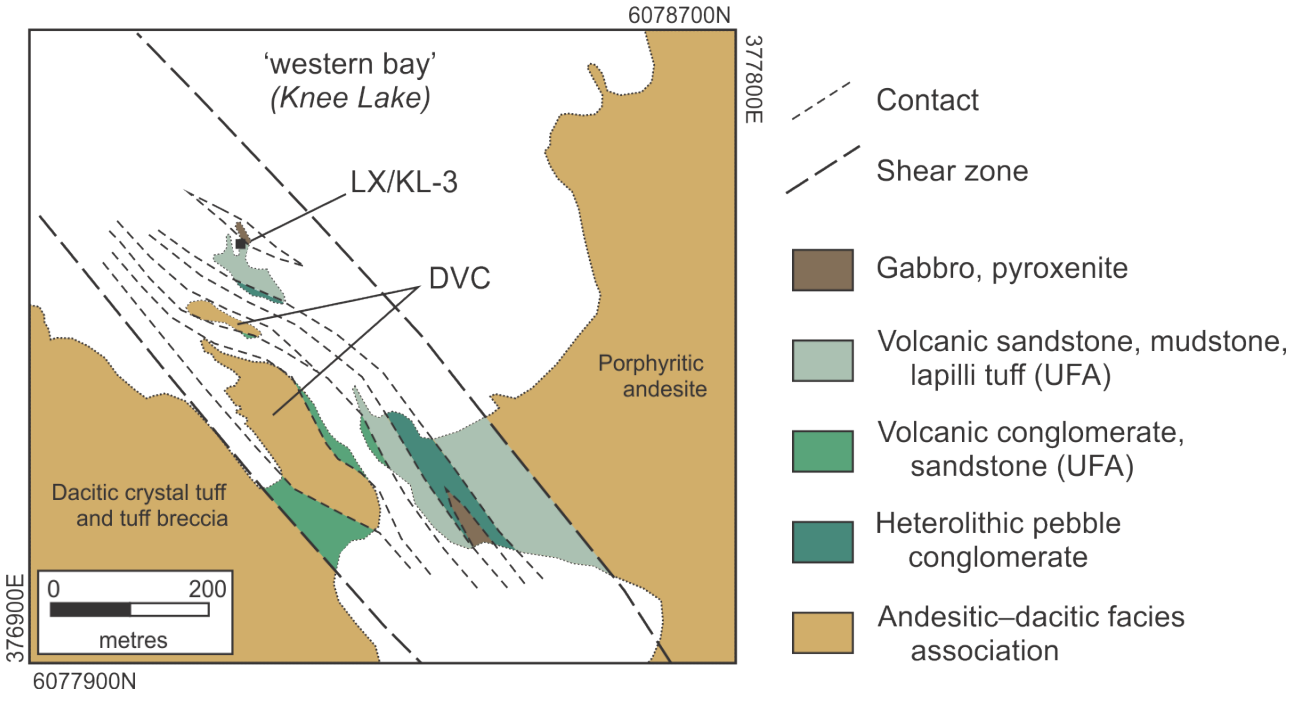

Figure 4: *Detailed map of the western bay showing thick lenses of dacitic volcanic conglomerate (DVC) of the andesitic–dacitic facies association interstratified with volcanic conglomerate, sandstone, mudstone and lapilli tuff of the ultramafic facies association (UFA).*

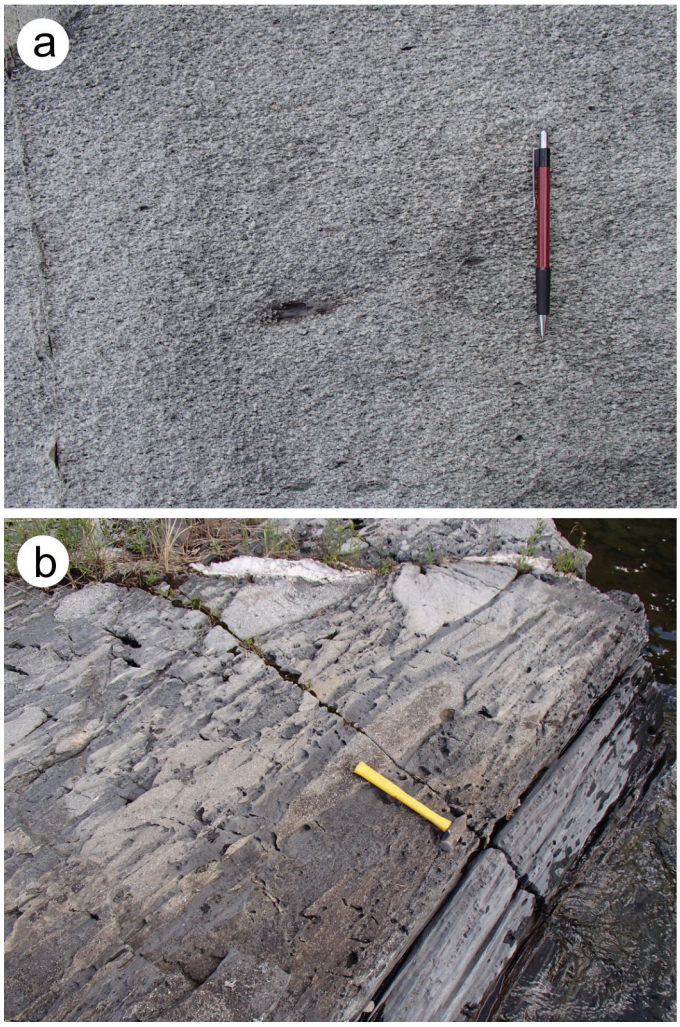

Figure 5: *Outcrop photographs of representative facies of the andesitic–dacitic facies association along the shoreline of Knee Lake west of the western bay:* ***a)*** *dacitic crystal tuff;* ***b)*** *dacitic tuff-breccia and crystal tuff.*

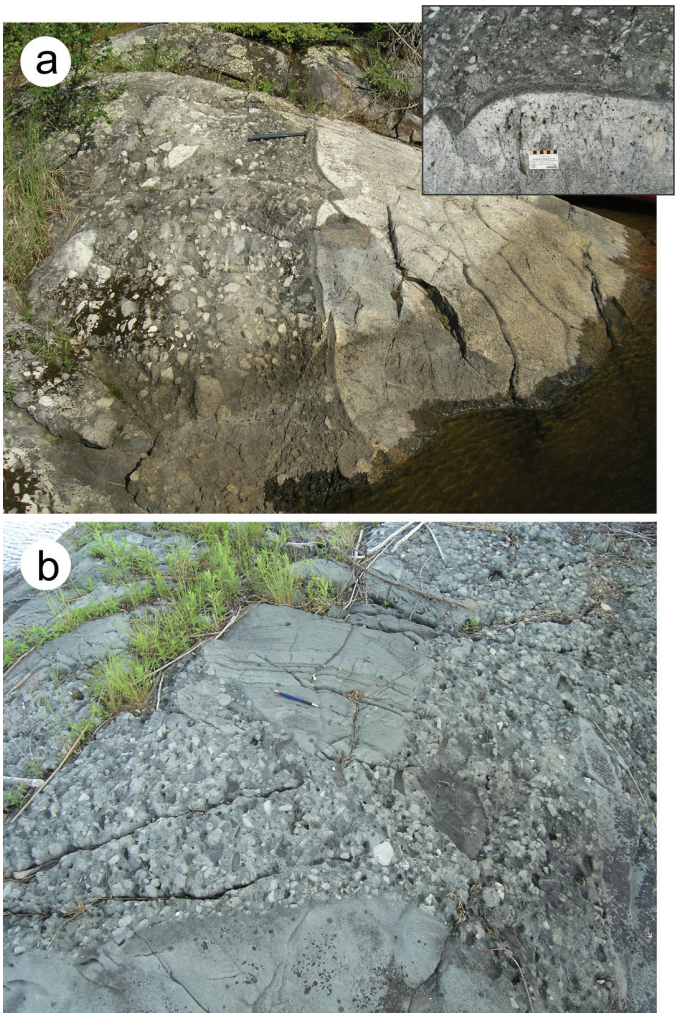

Figure 6: *Outcrop photographs of representative facies of the basaltic andesite facies association along the southern shoreline of the eastern bay:* ***a)*** *massive flow or cryptoflow of coarsely plagioclase-phyric basaltic andesite of shoshonitic affinity (hammer for scale along contact); inset shows the chilled and amygdaloidal margin of the flow;* ***b)*** *polymictic conglomerate containing large angular blocks of sandstone and gabbro (pencil for scale on large boulder of bedded sandstone).*

Of particular note in these conglomerates is a distinct population of near-spherical pebbles consisting of a lithic core of highly variable texture and composition mantled by a rim of fine grained, dark green, possibly tuffaceous, lithic material (Figure 9a, b). These composite particles vary in abundance from bed to bed but locally account for close to 5% of the clast population and range up to several centimetres in diameter, particularly in the eastern bay. Similar particles, referred to as 'pelletal lapilli', are common features of diatreme pipes formed by high-intensity explosive eruptions of volatile-charged melts, including kimberlites and other types of alkaline volcanic rocks. Recent work on pelletal lapilli from kimberlite pipes in South Africa indicates that these particles form when volatile-rich melts are emplaced into unconsolidated volcaniclastic material near the root zones of diatreme pipes and undergo intensive degassing, leading to a process referred to as 'fluidized spray granulation' (Gernon et al., 2012). Hence, the pelletal lapilli may derive from a volcanic centre that included one or more diatreme pipes. In this context, the lithic cores could represent local basement that was entrained in ascending magmas, or material that was eroded from vent walls during an explosive volcanic eruption. The diamondiferous sample LX/KL-2 contains 2–3% pelletal lapilli.

The thickest and coarsest beds of conglomerate occur along the southwest margin of the UFA in both the western and eastern bays. In the western bay, these include very thick (up to 75 m; Figure 4) lenses of crudely stratified, clast-supported, volcanic conglomerate that consists of very coarse (up to 50 cm) angular to rounded clasts of porphyritic dacite (Figure 10a) in a matrix of similar composition. Basal bed contacts are sharp and include abundant rip-ups of underlying sandstone and mudstone of the UFA (Figure 10b). Some beds of dacitic volcanic conglomerate contain angular blocks up to 2 m across of sandstone and conglomerate derived from the UFA (Figure 10c), indicating minimal transport and deposition via slumping or sliding of weakly consolidated material. Thin lenses of dacite-cobble conglomerate are interstratified with sandstone and mudstone of the UFA (Figure 10d), and the composition of

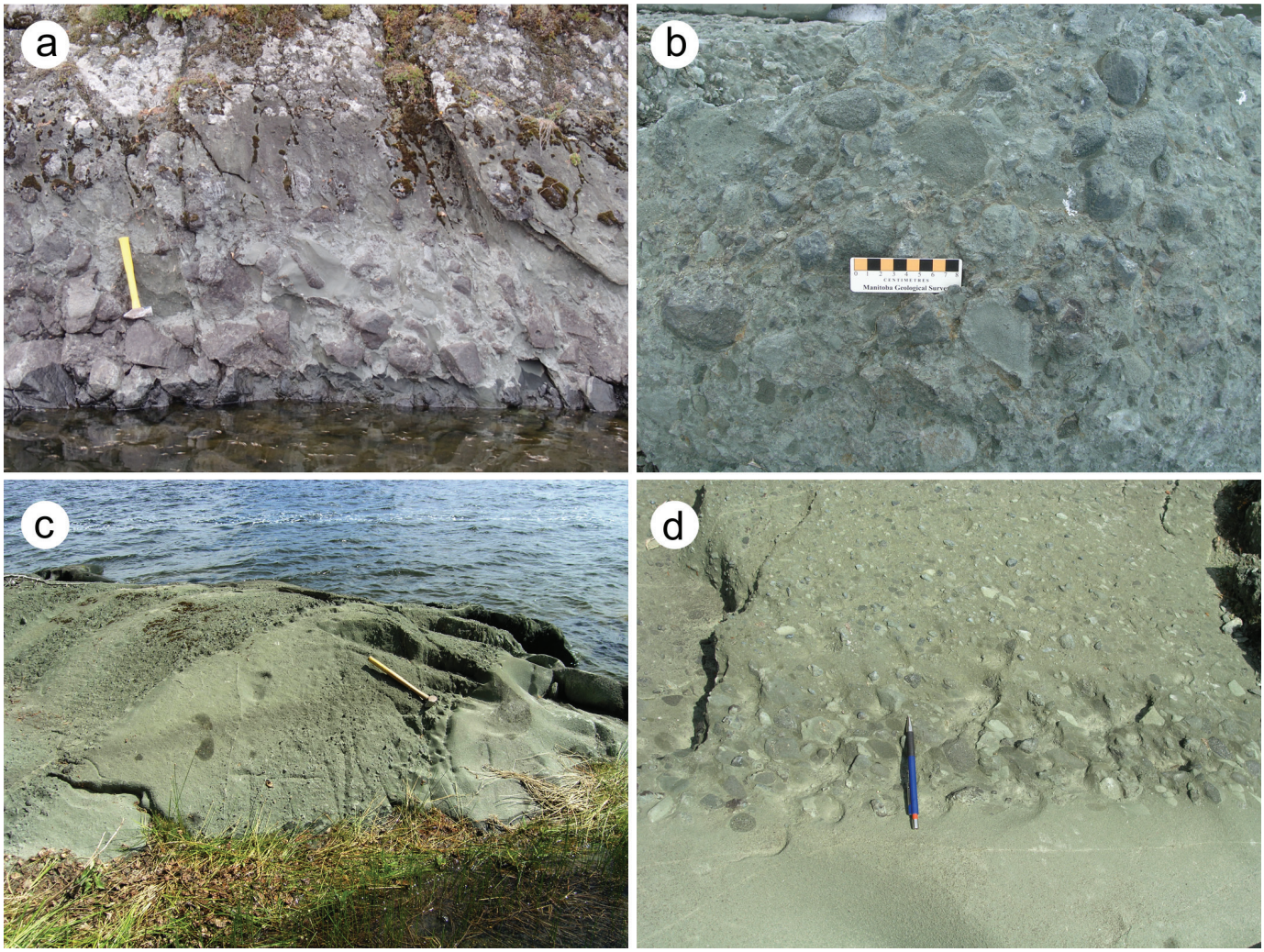

Figure 7: *Outcrop photographs of polymictic conglomerate of the ultramafic facies association:* ***a)*** *coarse boulder–cobble conglomerate containing angular clasts of basalt and abundant intraformational clasts of sandstone and conglomerate (e.g., behind hammer), western bay;* ***b)*** *massive cobble–pebble conglomerate showing polymictic clast population and well-rounded clasts, eastern bay;* ***c)*** *cobble–pebble conglomerate beds showing normal size grading and deeply scoured basal contacts, diamondiferous locality, eastern bay;* ***d)*** *detail of normally-graded bed of polymictic conglomerate, diamondiferous locality, eastern bay.*

the matrix becomes increasingly ultramafic (actinolite-chlorite) up-section.

Collectively, these features are suggestive of proximal channel-fill deposits in alluvial or shallow-marine fans, with material contributed from both dacitic and ultramafic (lamprophyric) sources, with the latter becoming prevalent up-section. Clasts of ultramafic–mafic volcanic and plutonic rocks in the conglomerates of the UFA may have been eroded from exposed basement (i.e., HRG; Syme et al., 1997) or, given the alkaline composition of the matrix and the presence of pelletal lapilli, may have been entrained in primitive alkaline magmas on their ascent to surface and liberated during eruptive or post-eruptive processes. In the former scenario, the conglomerates would be of mixed provenance, whereas in the latter scenario they could derive from a single source (i.e., an alkaline eruptive centre built upon a basement of HRG volcanic and intrusive rocks).

Ultramafic facies association – upper sections

The conglomerate of the UFA is interstratified at various scales with sandstone of similar composition, which is the dominant rock type in the upper sections of the UFA in both the eastern and western bays. This sandstone is bright olive green and pebbly, with a felted matrix of fine-grained chlorite and actinolite, and minor phlogopite/biotite, calcite, epidote, and accessory opaque minerals. Massive to faintly stratified beds of pebbly sandstone range up to several metres thick, particularly in the eastern bay, and have deeply scoured bases and normally graded tops capped by thin mudstone layers; some layers are convolute due to dewatering or slumping of unconsolidated material (Figure 11a). Intervals of fine to medium-grained, planar-bedded sandstone show turbidite bedforms, including scoured bases, normal size-grading, ripples and load structures (Figure 11b). Many beds contain contorted rip-up clasts of mudstone (Figure 11c), whereas other beds show diffuse compound size grading or tabular-planar crossbeds (Figure 11d), suggestive of rapidly changing sediment flow regimes. These features are interpreted to indicate deposition in a channelized shallow-marine fan setting.

In the western bay, the sandstones are locally interstratified with lapilli tuff and minor lapillistone (Figure 12a), which

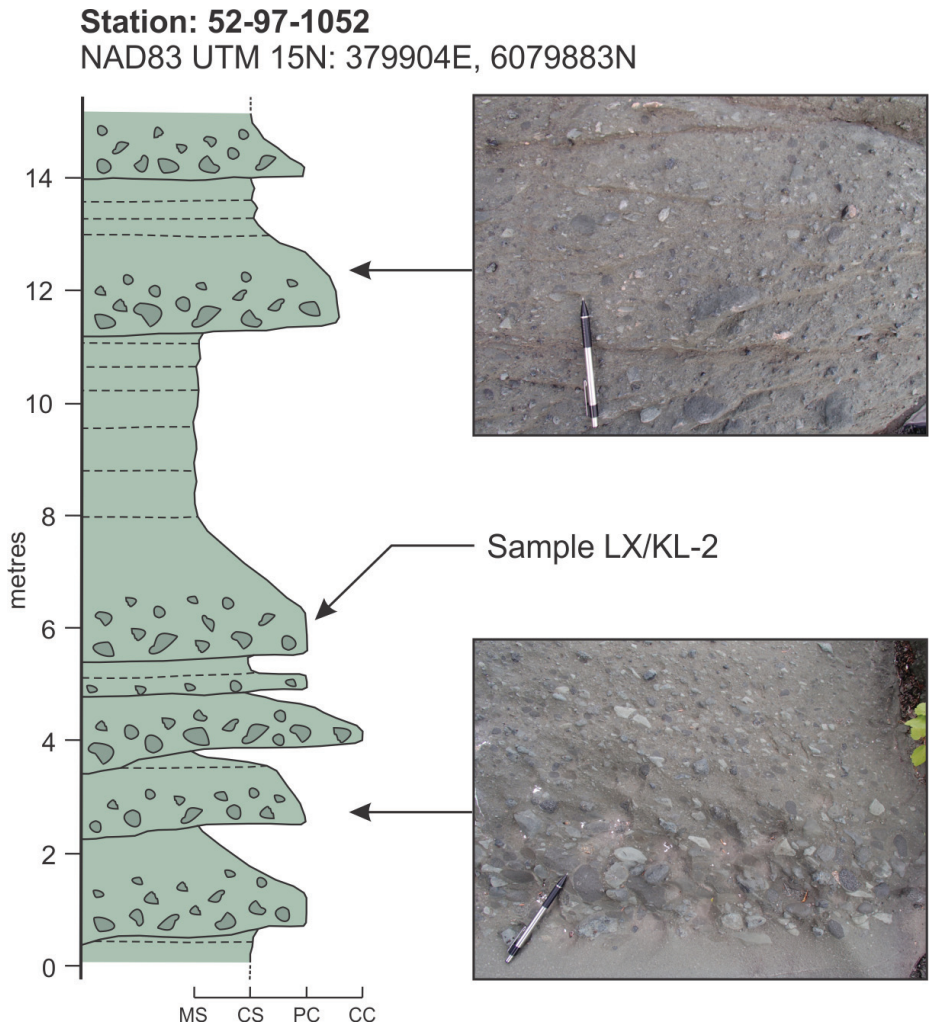

Figure 8: *Simplified stratigraphic column for bedded polymictic conglomerate at the diamondiferous locality (sample LX/KL-2) in the eastern bay. The outcrop consists of a series of thick, normally-graded beds of polymictic conglomerate that have scoured basal contacts and are capped by massive or crudely bedded (dashed lines) pebbly sandstone, consistent with sedimentation from high-density turbidity currents. Abbreviations: CC, cobble conglomerate; CS, coarse-grained sandstone; MS, medium-grained sandstone; PC, pebble conglomerate.*

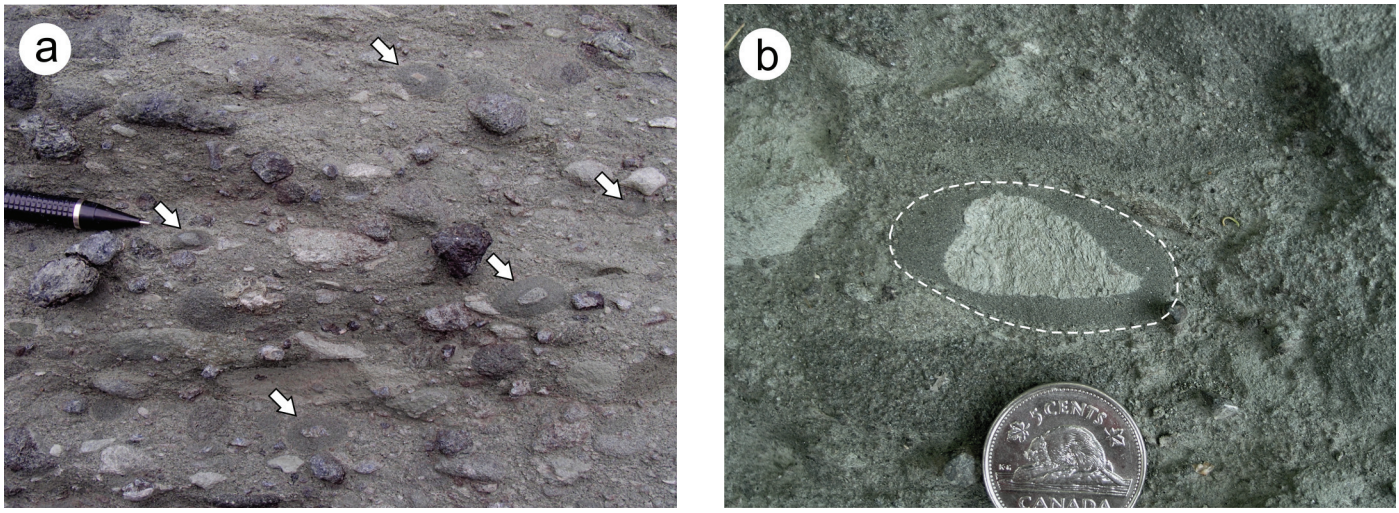

Figure 9: *Outcrop photographs of pelletal lapilli from the diamondiferous polymictic conglomerate locality in the eastern bay:* ***a)*** *pebble conglomerate bed containing abundant pelletal lapilli (arrows);* ***b)*** *detail of lapillus (dashed outline), showing serpentinite core and lithic rim in a matrix of pebbly sandstone.*

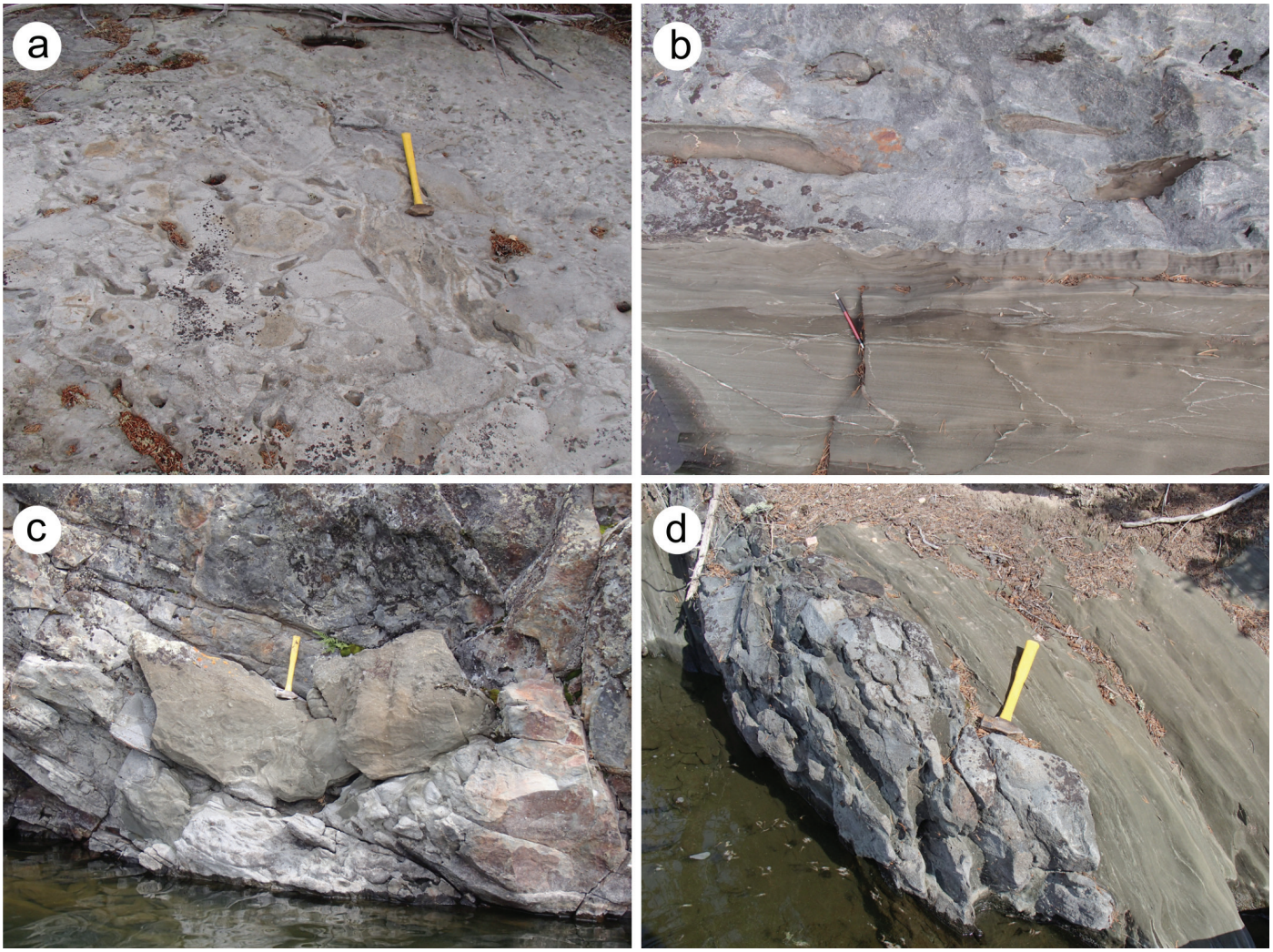

Figure 10: *Outcrop photographs of dacitic volcanic conglomerate that is interstratified with the UFA in the western bay:* ***a)*** *massive to crudely stratified, clast-supported, volcanic conglomerate;* ***b)*** *sharp basal contact of a thick lens of massive volcanic conglomerate, showing rip-ups of chloritic sandstone and mudstone derived from the underlying UFA;* ***c)*** *massive volcanic conglomerate containing a large angular block of pebble conglomerate derived from the UFA (below hammer);* ***d)*** *thin lens of dacite-cobble conglomerate interstratified with chloritic sandstone and mudstone of the UFA.*

form massive or crudely graded beds up to 3 m in thickness. Lithic lapilli are aphyric or sparsely porphyritic (phlogopite/biotite±pyroxene), with an aphanitic to very fine grained chlorite-actinolite groundmass, and are supported in a matrix of similar composition. Lapilli range from very angular and shard like to subround, with some having ragged cuspate margins and densely packed vesicles filled with carbonate (Figure 12b). These beds are essentially monolithic, in marked contrast to the conglomerate, although rare clasts of gabbro or felsic volcanic material occur locally. They are interpreted to represent primary pyroclastic deposits and may indicate periodic influxes of volcaniclastic material into the submarine fan during major eruptive events. Sample LX/KL-3 was collected from a graded bed of lapilli tuff approximately 3 m thick.

Whole-rock geochemistry

Representative samples were collected from all major supracrustal map units and subvolcanic intrusions during MGS mapping at Knee Lake and were submitted for geochemical analysis. Each sample consisted of least-altered homogeneous rock that was trimmed by hammer in the field to remove weathered surfaces, veins, altered fractures or other inhomogeneities. Clean rock chips were crushed and pulverized at the Midland Laboratory and Rock Storage Facility (Winnipeg, Manitoba), and homogenized powders were submitted to Activation Laboratories Ltd. (Ancaster, Ontario) for analysis. The powders were taken into solution by lithium metaborate-tetraborate fusion followed by nitric-acid digestion, with analysis by inductively coupled plasma–emission spectrometry for major elements and some trace elements (Ba, Sc, Sr, V, Y, Zr) and inductively coupled plasma–mass spectrometry for trace and rare earth elements.

The geochemical attributes of the UFA are described briefly below, including samples of sandstone, lapilli tuff and clasts of various types from conglomerate. Included for comparison purposes are samples of lamprophyre dikes from Knee

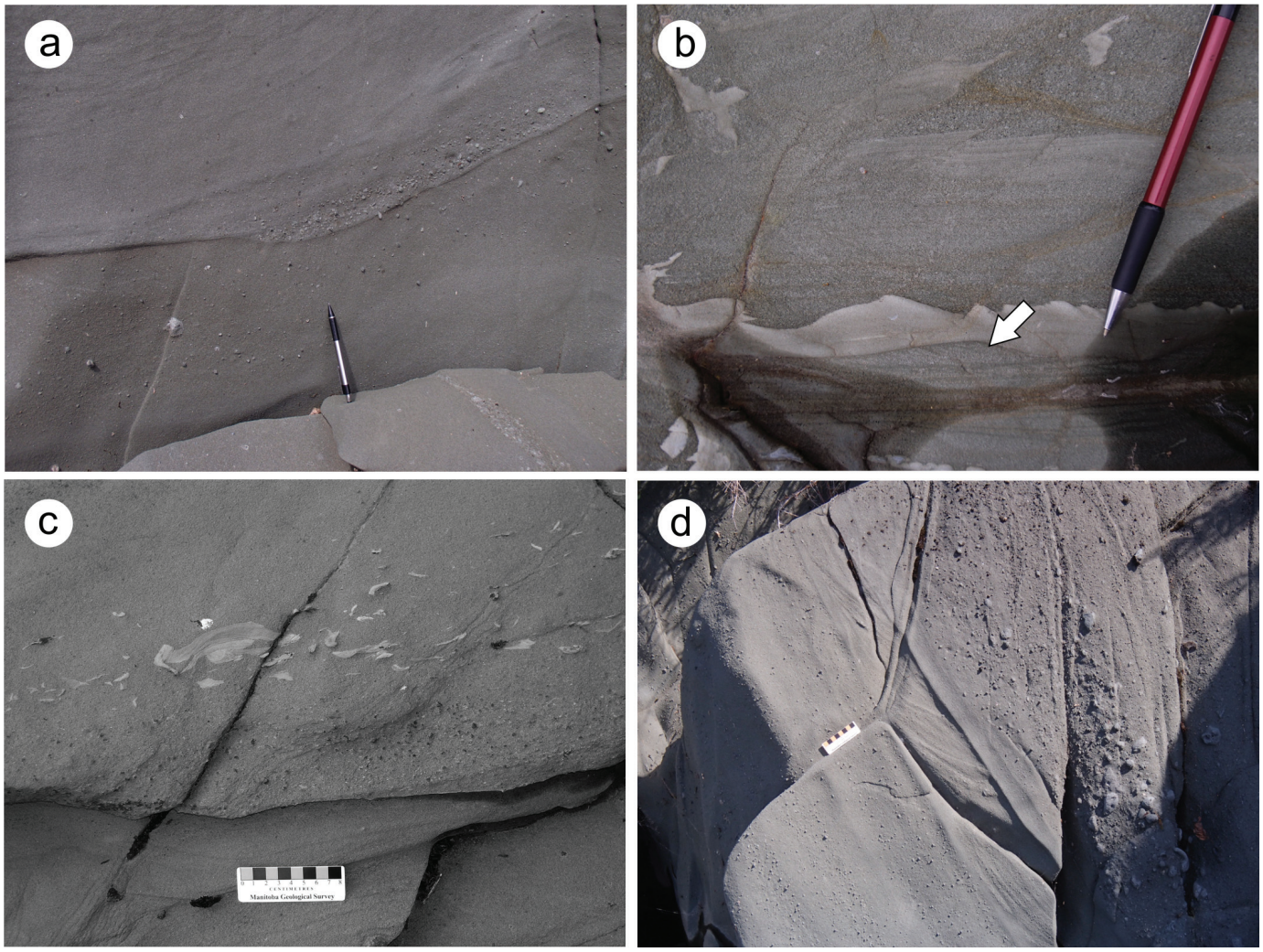

Figure 11: *Outcrop photographs of sandstone in the upper section of the UFA:* ***a)*** *massive pebbly sandstone showing scour-and-fill channel at the base and convolute bedding at the top, eastern bay;* ***b)*** *turbiditic sandstone and mudstone, showing normal size-grading, load structures, ripples (arrow) and mudstone rip-up clasts, western bay; bedding is overturned in this location; pencil points north;* ***c)*** *normally-graded sandstone bed with contorted rip-up clasts of mudstone, eastern bay;* ***d)*** *diffuse compound size-grading and cross-bedding in pebbly sandstone and conglomerate, eastern bay.*

Lake and Oxford Lake—the only rocks identified to date in the region that are chemically comparable to the UFA. Whole-rock geochemical data is provided in Appendix A.

Ultramafic facies association

Sandstone of the UFA is ultrabasic and shows evidence of alkaline affinity (43.7–45.3 wt. % SiO_2; 1.2–3.3 wt. % K_2O; Figure 13a). It is characterized by primitive compositions (16.7–18.7 wt. % MgO; >500 ppm Cr; >684 ppm Ni; Figure 13b, c), yet also shows significant enrichments in large-ion lithophile elements (LILE), with 332–1255 ppm Ba, 188–548 ppm Sr, and 42–132 ppm Rb (not plotted). Chondrite normalized rare earth element (REE) profiles are smooth and moderately sloped (La/Yb_{cn} = 3.8–6.1; Figure 13d, 14a), whereas primitive mantle normalized trace element profiles show depleted Nb, Zr and Ti (Figure 14b). Mutually overlapping profiles indicate a relatively uniform composition, perhaps due to homogenization by sedimentary reworking.

Lapilli tuff of the UFA is also ultrabasic (45.2 wt. % SiO_2), with a very primitive composition (18 wt. % MgO, 1450 ppm Cr, 480 ppm Ni), and shows evidence of alkaline affinity (2 wt. % K_2O, 303 ppm Ba, 126 ppm Sr, 69 ppm Rb; Figures 13a–d). The chondrite normalized REE profile is relatively flat (La/Yb_{cn} = 1.6), consistent with a depleted mantle source (Figure 14a). The primitive mantle normalized trace element profile is likewise relatively flat, with depleted Nb, Zr and Ti (Figure 14b).

Clasts of plutonic and volcanic material from conglomerate beds in the eastern bay show a general trend from alkaline basalt to subalkaline basaltic andesite (46.3–53.8 wt. % SiO_2; 0.3–2.6 wt. % K_2O; Figure 13a). Chondrite normalized profiles (Figure 14c) are smooth and vary from weakly depleted to moderately enriched in light rare-earth elements (LREE). In detail, three distinct profiles are apparent: relatively flat profiles with weakly depleted (La/Yb_{cn} = 0.8–1.0) or enriched (La/Yb_{cn} = 1.4–1.9) LREE, and moderately sloped profiles with enriched LREE (La/Yb_{cn} = 3.9–13.7). Primitive mantle normalized profiles (Figure 14d) for the latter group of samples are moderately-sloped, with depleted Nb, Zr and Ti, typical of profiles for modern volcanic-arc rocks. Profiles for the other samples have less pronounced negative Nb and Ti anomalies,

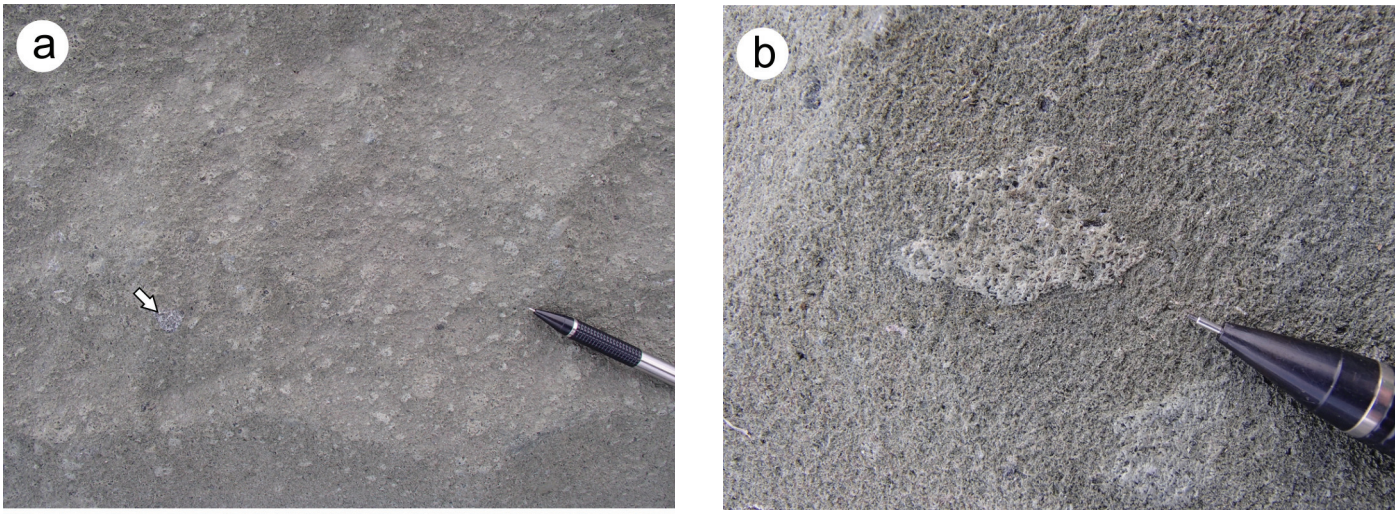

Figure 12: *Outcrop photographs of a thick (~3 m) bed of lapilli tuff in the western bay:* ***a)*** *matrix-supported lapilli tuff showing the essentially monolithic character (gabbro clast indicated by arrow);* ***b)*** *detail of lapillus showing ragged, cuspate margin and vesicular internal texture.*

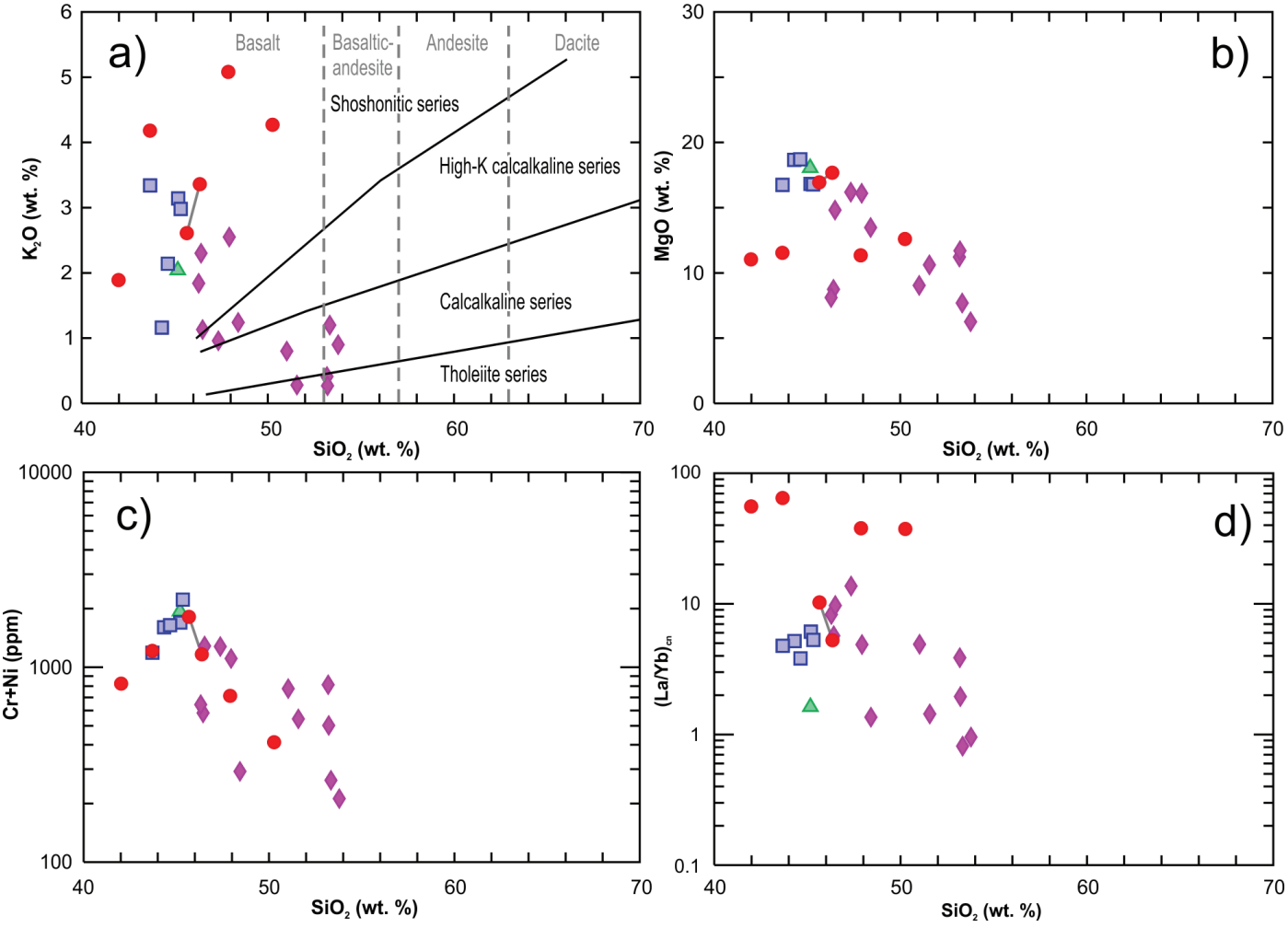

Figure 13: *Whole-rock geochemical data for various components of the UFA (sandstone, blue squares; lapilli tuff, green triangle; clasts in conglomerate, purple diamonds), including for comparison purposes examples of primitive lamprophyre dikes from Oxford Lake and Knee Lake (red circles; grey tie-lines indicate 'Type 1' dikes; see text for discussion);* ***a)*** *SiO_2 vs. K_2O; fields for shoshonitic, high-K calcalkaline, calcalkaline and tholeiitic series are from Peccerillo and Taylor (1976);* ***b)*** *SiO_2 vs. MgO;* ***c)*** *SiO_2 vs. sum of Cr+Ni;* ***d)*** *SiO_2 vs. $(La/Yb)_{cn}$ (cn, chondrite normalized; values of Sun and McDonough, 1989).*

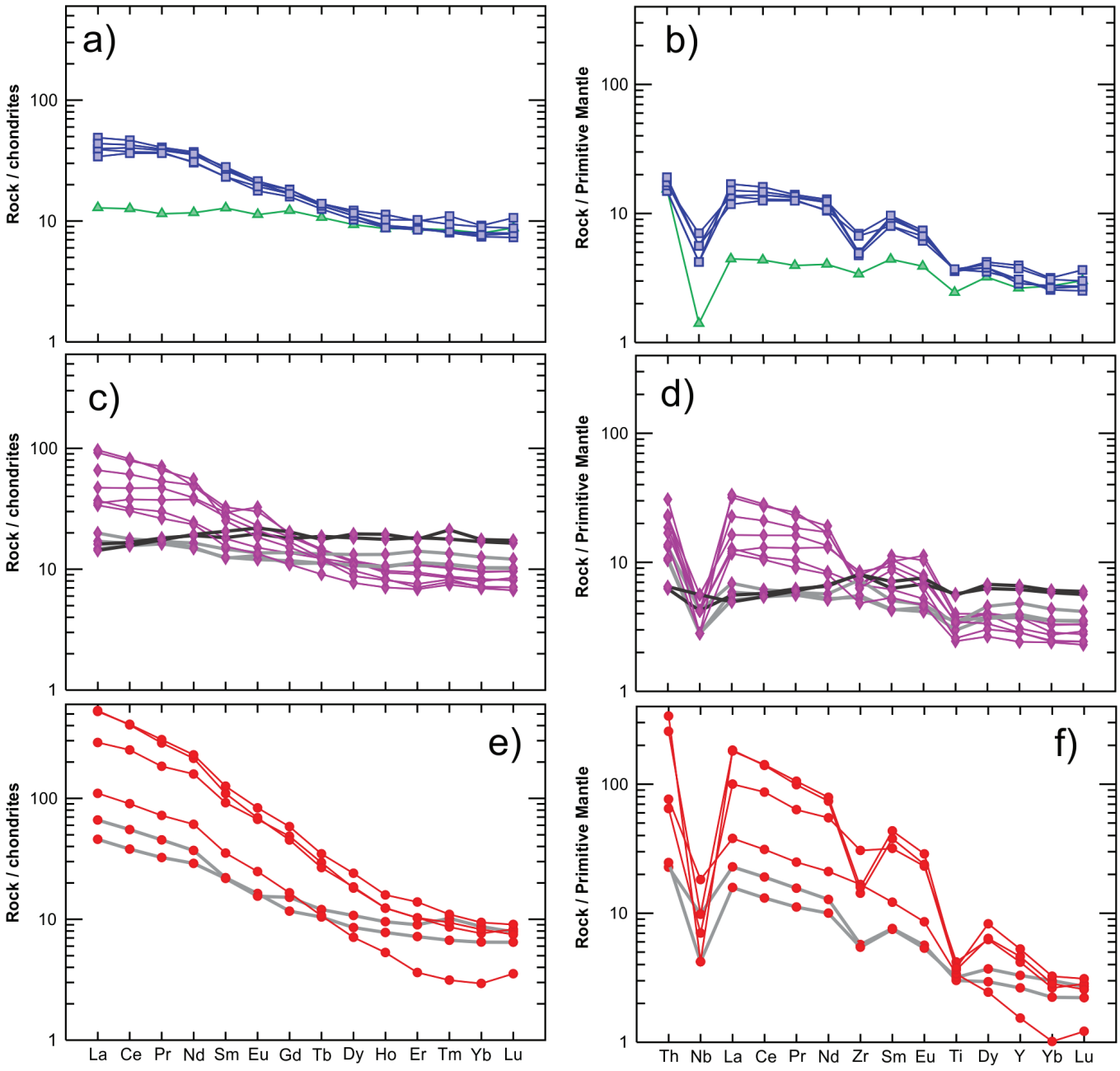

Figure 14: *Chondrite and primitive mantle–normalized trace-element diagrams for the various components of the UFA, including for comparison purposes examples of lamprophyre dikes from Oxford Lake and Knee Lake (symbols as in Figure 13);* ***a)*** *and* ***b)*** *sandstone and lapilli tuff;* ***c)*** *and* ***d)*** *clasts in conglomerate (different coloured tie-lines indicate the three different profiles evident in this sample set);* ***e)*** *and* ***f)*** *lamprophyre dikes (grey tie-lines indicate 'Type 1' dikes; see text for discussion). Normalizing values and order are from Sun and McDonough (1989).*

and slightly positive Zr, comparable to modern primitive-arc basalts. The most primitive clasts have compositions that are similar to the volcanic sandstone matrix, but typically have more fractionated LREE and more pronounced negative Nb anomalies (Figure 14a–d). On geochemical discrimination diagrams of immobile trace elements (e.g., Figure 15a), the samples define a fairly continuous trend from normal mid-ocean ridge basalt to evolved calcalkaline arc basalt. A steep trend of increasing Th/Yb at near constant Nb/Yb indicates significant crustal input (Figure 15b), also characteristic of modern volcanic-arc settings (Pearce and Peate, 1995; Pearce, 2008). These trends are comparable to those defined by basaltic rocks of the HRG at Oxford Lake and Knee Lake, which supports the notion that the clast population in the UFA was derived from local basement, either through erosion of exposed HRG or erosion of younger alkaline volcanic rocks that contained xenoliths of the HRG.

Lamprophyre dikes

Lamprophyre dikes at Oxford Lake and Knee Lake have a wide range of compositions and show a general trend from ultrabasic and alkaline to intermediate and high-K calcalkaline varieties (Anderson, 2016a). In order to facilitate comparisons

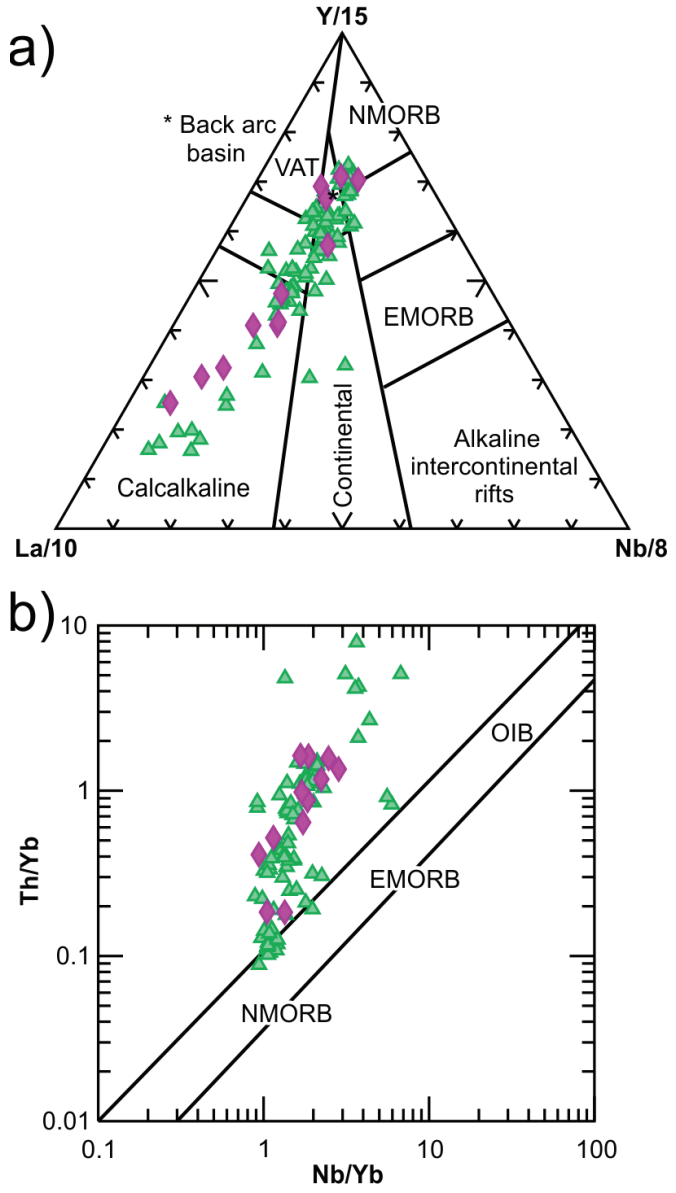

Figure 15: *Trace element discrimination diagrams for clasts in conglomerate of the UFA (purple triangles), shown in comparison to mafic volcanic rocks of the HRG at Oxford Lake and Knee Lake (green triangles; unpublished data from Syme et al., 1997, 1998; Anderson et al., 2012, 2013):* ***a)*** *La/10 vs. Y/15 vs. Nb/8 (Cabanis and Lecolle, 1989);* ***b)*** *Log Nb/Yb vs. Log Th/Yb (Pearce and Peate, 1995; Pearce, 2008). Abbreviations: EMORB, enriched mid-ocean–ridge basalt; NMORB, normal mid-ocean–ridge basalt; OIB, ocean-island basalt; VAT, volcanic-arc tholeiite.*

with the relatively primitive rocks of the UFA, the geochemical characteristics of only the most primitive lamprophyre dikes (>11 wt. % MgO) are described in detail below; these are the only rocks in the Oxford Lake–Knee Lake belt that have similar bulk compositions to the UFA.

The primitive lamprophyre dikes vary in bulk composition from ultrabasic to basic (42–50.3 wt. % SiO_2) and are strongly alkaline (1.9–5.1 wt. % K_2O; Figure 13a); they include two distinct geochemical types. Type 1 dikes (n = 2) are characterized by more primitive compositions, with 16.9 and 17.7 wt. % MgO and high concentrations of Ni and Cr (>1200 ppm combined), whereas Type 2 dikes (n = 4) are less primitive, with 11–12.6 wt. % MgO and less than 1200 ppm combined Ni and Cr (Figure 13b, c). Type 1 dikes have lower concentrations of LILE (<658 ppm Ba; <144 ppm Rb; <273 ppm Sr), but unusually high concentrations of Cs (145 and 174 ppm). Chondrite normalized REE profiles are smooth and less sloped (La/Yb_{cn} = 5.3 and 10.2), and primitive mantle normalized profiles show moderate depletions of Nb, Zr and Ti (Figure 14e, f). Type 2 dikes have higher concentrations of LILE (>736 ppm Ba; >76 ppm Rb; >310 ppm Sr), but lower Cs contents (6–18 ppm). Chondrite normalized REE profiles are smooth and comparatively steep (La/Yb_{cn} = 37.4–64.6); primitive mantle normalized profiles generally show much more pronounced depletions of Nb, Zr and Ti, and very strongly fractionated heavy REE (Figure 14e, f).

Discussion

With the exception of the unusual Cs contents, the primitive Type 1 lamprophyre dikes are compositionally similar to volcanic sandstone and lapilli tuff of the UFA, suggesting they may be different facies of the same volcanic association, with the lapilli tuff possibly representing primary volcaniclastic deposits from lamprophyric volcanism and the sedimentary rocks representing volcanic material that was reworked in subaerial and shallow-marine settings. No lamprophyre dikes are observed to cut the UFA, suggesting that such an association is permissible; geochronologic work is ongoing to resolve absolute ages. Arc-like geochemical signatures (depleted Nb, Zr, Ti; enriched Ba, K, Rb, Sr) and primitive bulk compositions of the Type 1 lamprophyres and volcaniclastic rocks point to a metasomatized mantle source, consistent with a supra-subduction–zone setting. The presence of microdiamonds in the conglomerate indicates erosion of rocks derived from the upper mantle, at depths greater than 140 km; however, given the polymictic character of sample LX/KL-2 and the processing methodology (see below), the specific host for the microdiamonds remains unknown. Type 1 lamprophyre dikes have not been processed for microdiamonds or indicator minerals.

Type 2 dikes are similar in terms of trace-element and rare-earth element geochemistry to more evolved shoshonitic volcanic rocks of the basaltic andesite facies association, as well as more evolved lamprophyre dikes (Anderson, 2016a), suggesting they represent a more primitive end-member of the alkaline volcanic suite. As described by Brooks et al. (1982) these rocks are comparable to modern shoshonite-series rocks formed in convergent margin settings. One of the Type 2 dikes cuts synorogenic sedimentary rocks at central Knee Lake, indicating that at least some of this lamprophyric magmatism post-dated deposition of the OLG, and must therefore be unrelated to the diamondiferous volcanic conglomerates of the UFA.

Structural geology

Map patterns, mesoscopic deformation structures and overprinting relationships indicate that supracrustal rocks at Knee Lake have been affected by at least five generations (G_1 to G_5) of deformation structures (Anderson et al., 2015b; Anderson, 2016b). Analysis of structural data collected in 2015, 2016 and

2017 is ongoing; in the interest of brevity and for the purpose of understanding map patterns and structural relationships of the various map units, only a brief summary of preliminary findings is provided here.

The earliest ductile structures are isoclinal F_1 folds and associated axial-plane S_1 foliations observed in bedded greywacke and iron formation in the OLG. Macroscopic isoclinal F_1 folds are inferred from bedding-cleavage relationships in several locations and from aeromagnetic patterns southwest of Knee Lake and in Opapuskitew Bay (Figure 2). The latter structure is defined by iron formation and appears to be truncated by the basal unconformity of the synorogenic sedimentary basin exposed along the Hayes River upstream of southern Knee Lake (Figure 2; see below).

Mesoscopic F_1 folds are overprinted by upright, open to isoclinal, steeply plunging F_2 folds (Figure 16a), which are parasitic to macroscopic F_2 folds that appear to control map patterns within the major structural panels. The F_2 folds are associated with a penetrative, axial-planar S_2 foliation that trends northeast to east-southeast and is subvertical. The S_2 foliation transects F_1 folds indicated by younging reversals in bedded greywacke and locally intensifies into a transposition fabric. A prominent S_2 shape-fabric defined by flattened primary features is the main fabric observed in most outcrops (outside of later shear zones) and includes a downdip L_2 stretching lineation that varies from oblate (pancake-shaped) to strongly prolate (cigar-shaped; Figure 16b). South of the TISZ, sigmoidal inclusion trails in garnet and cordierite porphyroblasts on the limbs of F_2 folds indicate that these structures likely formed during peak metamorphism (Anderson et al., 2015b).

Younging reversals and local structural overturning in the UFA indicate the presence of macroscopic folds, which are interpreted to represent F_2 structures. In the eastern bay, bedding and younging criteria define an upright, tight, macroscopic syncline that plunges shallowly to the east-southeast (Figure 17a). Only a limited number of bedding measurements are available for the UFA in the western bay, but these indicate that the section is overprinted by upright isoclinal folds that are overturned toward the southwest and plunge moderately to the northeast (Figure 17b). This section contains several mesoscopic examples of isoclinal fold closures (Figure 16c). These folds are associated with an axial planar foliation defined by actinolite and chlorite, and a weak to moderate shape-fabric defined by deformed clasts. The latter fabric includes a locally prominent down-dip L_2 stretching lineation (Figure 16d, 17c, d).

At southern and central Knee Lake, macroscopic F_2 folds do not carry across the basal contacts of the synorogenic sedimentary basins (i.e., macroscopic younging reversals are not observed in these rocks), which is taken to indicate that the F_2 folds are older. It is for this reason that the basal contact is interpreted to be an angular unconformity. These younger sedimentary rocks also contain a shape fabric and locally penetrative foliation but, in contrast to the older rocks, these are only associated with minor open folds. The upper contacts of these basins are defined by faults that are interpreted to represent thrusts (Anderson, 2016b). Collectively, these faults and fabrics are tentatively assigned to the G_3 generation of deformation structures and are interpreted to record renewed shortening subsequent to deposition of the fluvial-alluvial sedimentary rocks in localized synorogenic basins.

At southern Knee Lake, the macroscopic F_2 folds are disrupted by subvertical ductile shear zones that bound major and minor structural panels. The principal examples are the LISZ and TISZ, which mostly delimit the 'Southern Knee Lake shear zone' of Lin et al. (1998). These shear zones vary in trend from northeast to southeast; at present it is unknown whether they all represent a single generation of structure, but they are assigned here to the G_4 generation on the basis of similar style and kinematics of fabrics. Aligned minerals and attenuated primary features define a penetrative, often mylonitic, S_4 foliation; in some outcrops the shear zones include wide zones of layered tectonite formed via intense transposition of bedding or attenuation of large clasts. Elongate clasts define an L_4 stretching lineation that plunges shallowly to the northwest or southeast and is locally subhorizontal (Figure 16e; 17d). Shear-sense indicators (e.g., S-C fabrics, shear bands, asymmetric boudins) are locally well developed on horizontal surfaces and indicate dextral shear (Figure 16f). Open to isoclinal Z-folds, locally associated with a weak to moderate axial-planar crenulation cleavage, variably overprint the S_4 foliation and appear to result from progressive G_4 deformation. Systematic patterns of fabric orientations at southern Knee Lake were interpreted to result from deformation-path partitioning and progressive deformation within a kinematic regime of dextral transpression (Lin et al., 1998; Lin and Jiang, 2001); however, these fabrics may also result from separate deformations. In this scenario, the regional steep L_2 lineation may have been overprinted by the shallow L_4 lineation, localized within younger shear zones.

Later (G_5) structures include concordant to discordant, brittle-ductile or brittle faults, some of which are associated with narrow (<1 m) zones of cataclasite or pseudotachylite. A possible major structure of this type, which is defined by sharply truncated magnetic lineaments in the central portion of southern Knee Lake, trends east-northeast from Opapuskitew Bay to just south of Omusinapis Point. Although not observed in outcrop, this structure appears to account for the map patterns south of Pain Killer Bay, where several units show evidence of significant offset.

Indicator mineral and microdiamond results

Two samples of the UFA at southern Knee Lake were collected in July 2016 for microdiamond and indicator mineral processing. Sample LX/KL-2 (31 kg) is from a bed of polymictic volcanic conglomerate (~2.5 m in thickness) in the eastern bay, whereas sample LX/KL-3 (33 kg) is from a layer of monolithic lapilli tuff (~3 m in thickness) in the western bay. The former was collected by sledge hammer, whereas the latter was collected using a rock saw with a diamond wet-blade. Both samples were processed at the Geoanalytical Laboratories of the Saskatchewan Research Council (Saskatoon, Saskatchewan). The sample prefixes 'LX' and 'KL' denote splits processed for microdiamonds and indicator minerals, respectively.

For microdiamond recovery, individual samples weighing approximately 8 kg were fused in a kiln containing caustic soda and the melt was poured through a stainless steel wire mesh with an aperture width of 0.075 mm. The oversize caustic residue

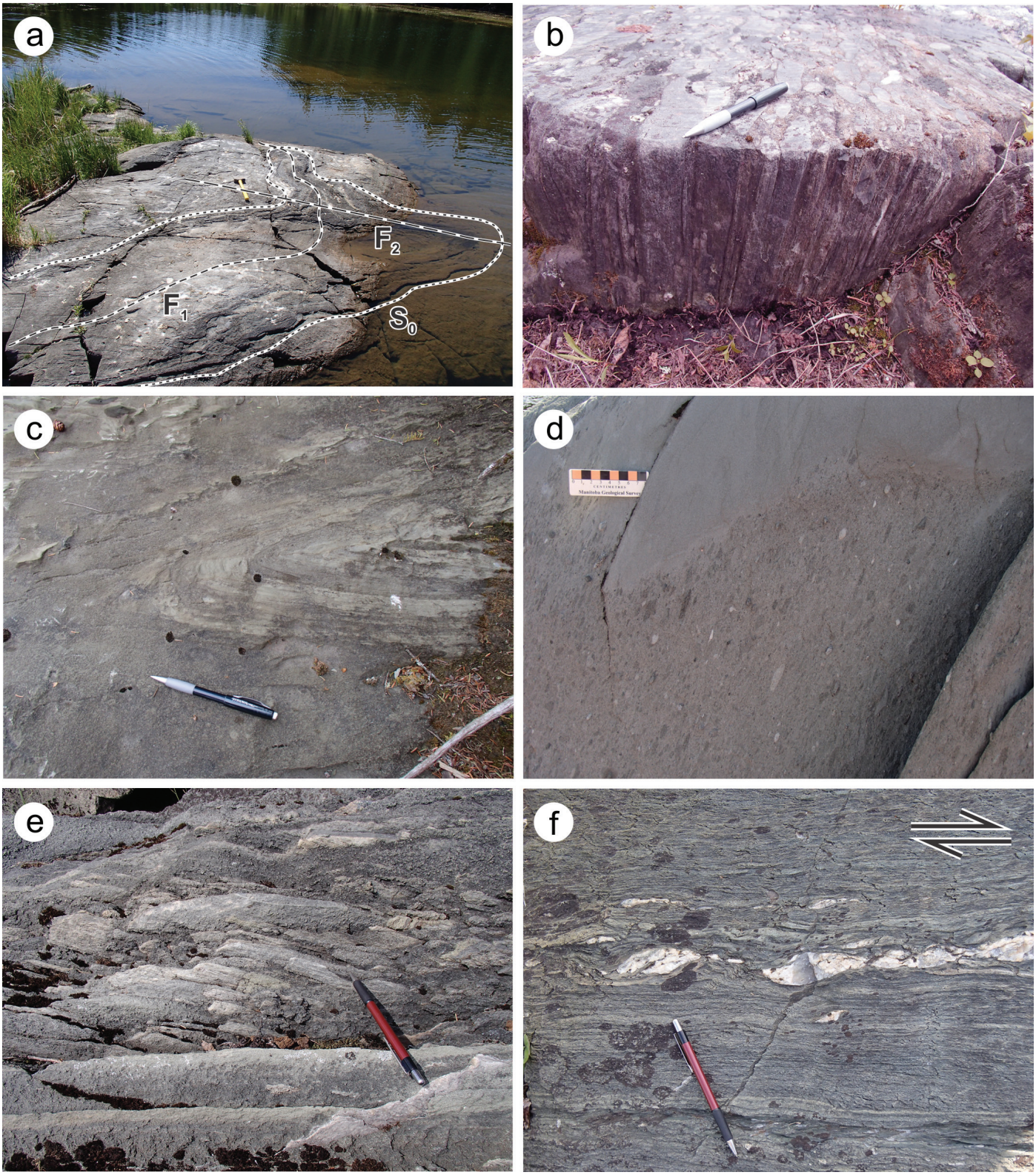

Figure 16: *Outcrop photographs of deformation structures at southern Knee Lake:* ***a)*** *isoclinal F_1 fold, defined by iron formation in greywacke ('S_o' indicates bedding), overprinted by F_2 folds (axial planes are indicated by dashed lines);* ***b)*** *steep L_2 stretching lineation in polymictic conglomerate; prolate fabric indicated by aspect ratios of clasts on the horizontal and vertical outcrop faces;* ***c)*** *isoclinal F_2 fold in bedded sandstone and mudstone of the UFA, western bay;* ***d)*** *vertical outcrop face showing steep stretching lineation (L_2) at a high-angle to bedding in the hinge of a mesoscopic F_2 fold in bedded conglomerate and sandstone of the UFA, western bay;* ***e)*** *shallow-plunging L_4 stretching lineation defined by the long axis of deformed clasts in volcanic conglomerate;* ***f)*** *mylonitic S_4 foliation and F_4 Z-folds in the Long Island shear zone (asymmetric quartz boudins indicate dextral shear).*

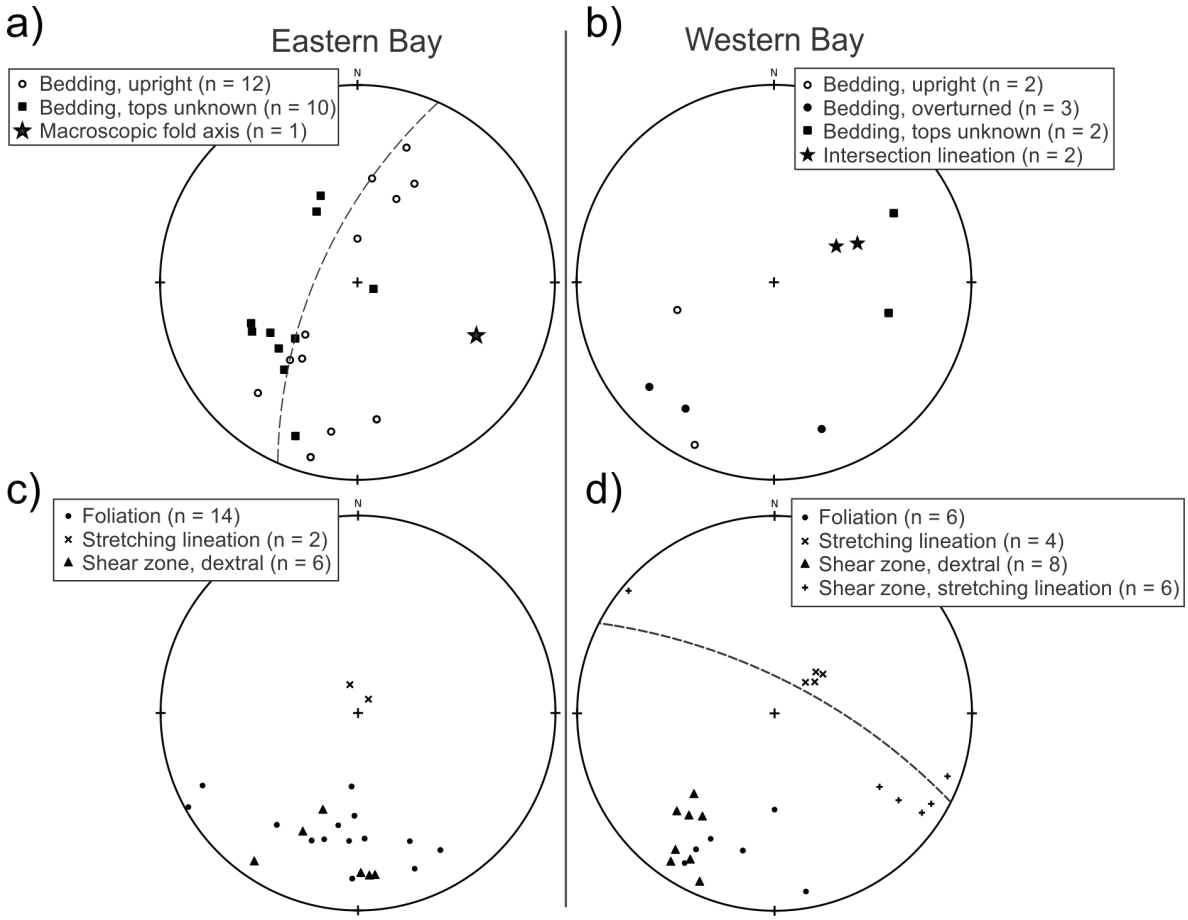

Figure 17: *Lower-hemisphere, equal-angle stereographic projections of structural data from the UFA:* ***a)*** *poles to bedding in the eastern bay; star represents pole to girdle (dashed line) defined by bedding orientations and indicates the plunge of the macroscopic F_2 fold;* ***b)*** *poles to bedding (S_0) in the western bay; stars indicate measured S_0-S_2 intersection lineations, corresponding to mesoscopic F_2 fold hinges;* ***c)*** *L_2 lineation and poles to planar fabrics (foliation is S_2; shear zones are S_4) in the eastern bay;* ***d)*** *L_2 (steep) and L_4 (shallow) lineations and poles to planar fabrics (foliation is S_2; shear zones are S_4) in the western bay.*

was chemically treated to reduce the sample volume and the resulting material was screened into standard size fractions, followed by optical observation and recovery of microdiamonds. Synthetic tracer diamonds were included in each sample run to monitor the quality of the method. Recovered natural microdiamonds were individually described and measured, and weighed with an externally calibrated microbalance.

Indicator minerals were recovered by crushing (60% passing a 2 mm screen), followed by dry sieving into size fractions (<0.25 mm, 0.25–0.5 mm, 0.5–1.0 mm and 1.0–2.0 mm), and magnetic and heavy liquid separation of the 0.25–0.5 mm and 0.5–1.0 mm fractions. The heavy fractions (>2.96 specific gravity) underwent further magnetic separation, followed by optical screening. Indicator minerals were analyzed for major elements and select trace elements (Nb, Ni, V, Zn) using a Cameca SX-100 electron probe micro-analyzer at the Geoanalytical Laboratories of the Saskatchewan Research Council (Saskatoon, Saskatchewan). Indicator mineral geochemical data is provided in Appendix B.

Indicator minerals

As shown in Table 1, sample KL-2 (6.42 kg) yielded 52 indicator mineral grains, including chromite, Cr-spinel and tourmaline, whereas sample KL-3 (5.35 kg) yielded 70 grains, including chromite, Cr-diopside, Cr-spinel, olivine (forsterite) and amphibole (hornblende). Because of the processing methodology (bulk-rock), the relative contribution of clasts vs. matrix to the recovered indicator mineral population is unknown. In addition, the morphology of individual grains and any internal variability in structure, texture or composition (e.g., overgrowths, reaction rims, primary zoning, etc.) have yet to be characterized. In the case of the compositional data for spinel, for example, it is therefore not possible from the present dataset to differentiate between xenocryst, macrocryst or groundmass spinel. Hence, the analysis below should be considered preliminary.

Chromite and Cr-spinel

As noted above, both samples contain abundant grains of chromite (>30 wt. % Cr_2O_3) and lesser grains of Cr-spinel (>45 wt. % Cr_2O_3, >10 wt. % MgO), including 3 grains of diamond-inclusion Cr-spinel (>60 wt. % Cr_2O_3, >10 wt. % MgO) that were recovered from sample KL-3. Spinel grains from both samples typically have low MgO concentrations (<2 wt. %), but show a compositional scatter towards increasing MgO at near-constant Cr_2O_3 (Table 2; Figure 18a). Although the overall

Table 1: Summary of indicator mineral counts for samples KL-2 and KL-3.

Sample	Rock type	Chromite	Cr-spinel[1]	DI Cr-spinel[2]	Cr-diopside	Olivine	Amphibole	Tourmaline
KL-2	Conglomerate	47	4	–	–	–	–	1
KL-3	Lapilli tuff	31	6	3	27	2	1	–

[1] >45 wt. % Cr_2O_3, >10 wt. % MgO
[2] Diamond inclusion (DI); >60 wt. % Cr_2O_3, >10 wt. % MgO

Table 2: Summary of compositional ranges for spinel group minerals and Cr-diopside from samples KL-2 and KL-3.

Sample	Rock type	Chromite*		Cr-diopside	
		MgO (wt. %)	Cr_2O_3 (wt. %)	MgO (wt. %)	Cr_2O_3 (wt. %)
KL-2	Conglomerate	0.21–15.01	36.97–59.14	–	–
		n = 51			
KL-3	Lapilli tuff	0.23–17.14	33.73–62.38	16.55–17.93	0.41–1.06
		n = 40		n = 27	

* Includes Cr-spinel and diamond inclusion Cr-spinel

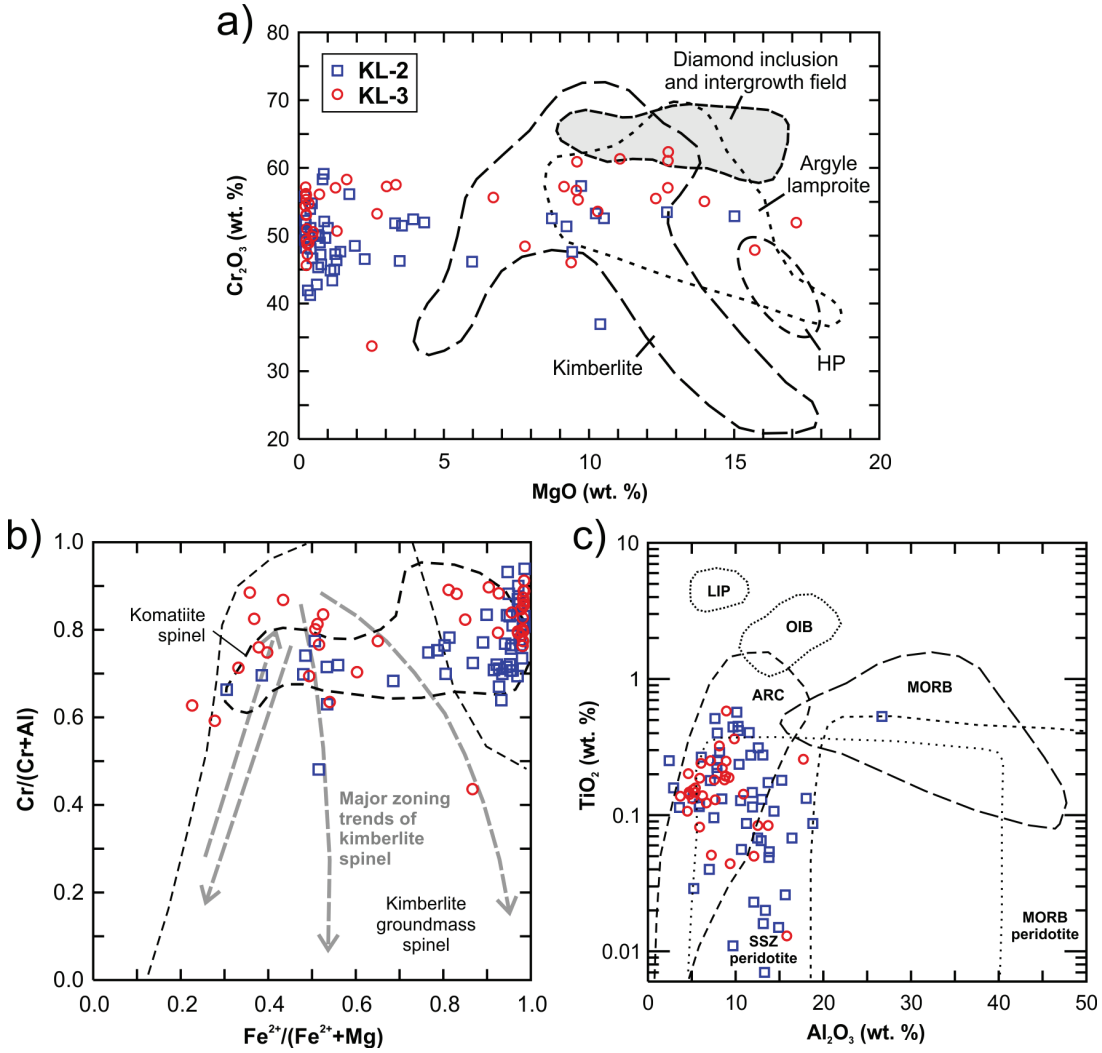

Figure 18: *Bivariate plots of compositional data for chromite and Cr-spinel grains recovered from samples KL-2 and KL-3:* ***a)*** *MgO vs. Cr_2O_3; fields for diamond inclusions, Argyle lamproite and HP lamprophyre are from Fipke et al. (1995); field for kimberlite spinel is from Nowicki et al. (2007);* ***b)*** *$Fe^{2+}/(Fe^{2+}+Mg)$ vs. Cr/(Cr+Al); compositional field for komatiite spinel is from Barnes and Roeder (2001); compositional field and principal zoning trends for kimberlite groundmass spinel are from Roeder and Schulze (2008);* ***c)*** *Al_2O_3 vs. TiO_2 (after Kamenetsky et al., 2001). Abbreviations: ARC, island-arc; LIP, large igneous province; OIB, ocean-island basalt; MORB, mid-ocean–ridge basalt; SSZ, supra-subduction zone.*

ranges and trends of spinel compositions are similar, subtle differences are also apparent, with the main population of spinel from sample KL-2 showing slightly higher MgO and lower Cr_2O_3. The majority of analyses fall outside the compositional fields for kimberlite and lamproite. Kimberlitic spinel in particular typically defines strong trends of decreasing Cr_2O_3 with increasing MgO, and scatter towards Cr- and Mg-poor compositions, neither of which are obvious in the Knee Lake samples. A weak trend of decreasing Cr_2O_3 with increasing MgO is apparent in Cr-spinel from sample KL-3, but the current dataset is insufficient to resolve this trend in detail.

On the $Fe^{2+}/(Fe^{2+}+Mg)$ vs. Cr/(Cr+Al) plot, the dataset also shows little evidence of the major compositional zoning trends identified by Roeder and Schulze (2008) for spinel from kimberlites and related rocks (Figure 18b). Most of the data points fall outside of the compositional range of kimberlite groundmass spinel, but overlap the compositional field for komatiite spinel (Figure 18b) defined by Barnes and Roeder (2001). On the Al_2O_3 vs. TiO_2 plot (Kamenetsky et al., 2001), chromite and Cr-spinel from both samples plot within the compositional fields for arc volcanic rocks and supra-subduction–zone peridotite (Figure 18c), suggesting that these minerals may have crystallized from 'typical' partial melts of mantle-wedge peridotite in a subduction setting.

Cr-diopside

Sample KL-3 contains a significant population of Cr-diopside grains, which are absent from sample KL-2. In general, these grains have very uniform compositions (16.6–17.9 wt. % MgO; 0.4–1.1 wt. % Cr_2O_3; Table 2), with moderate Mg numbers (87.2–89.7), and define short linear trends on Harker plots of major element oxides (not plotted). These Cr-diopside grains have Al_2O_3 and Cr_2O_3 concentrations typical of lithospheric mantle (garnet peridotite), and plot within the compositional field for Cr-diopside included in diamond (Figure 19). Although this sample was not diamondiferous, these data coupled with the presence of diamond-inclusion Cr-spinel indicate that the alkaline source magma for sample KL-3 may have been derived from within the diamond stability field.

Diamonds

Sample LX-2 consisted of two splits weighing 7.9 kg each, which yielded 66 and 78 microdiamonds (MD; n = 144; Table 3); no MD were recovered from sample LX-3. The MD from sample LX-2 are yellow (35%), off-white (32%), white (29%) or grey (4%); transparent (72%) or translucent (28%); contain minor (42%) or obvious (14%) inclusions; or are inclusion-free (44%). Fragments are most abundant (42%), although the population also includes cuboid, octahedral, dodecahedral and tetrahexahedral crystals, with cuboids being the dominant form (31%). Also present are irregular or twinned crystals (including 1 macle) and crystal aggregates. A significant proportion of the MD are polycrystalline (28%) and many show evidence of distortion (24%). Resorption features (Class 1–5) are apparent in a small population (14%) of the MD. The overall morphological features are compatible with cratonic diamonds as opposed to orogenic or phenocrystal diamonds, which tend to show little evidence of resorption, although the latter diamond types are also often small (<1 mm) in size (e.g., De Stefano et al., 2006). The largest MD (0.86 mm x 0.48 mm x 0.28 mm) is a white/colourless, transparent crystal fragment with minor inclusions that weighs 0.2071 mg (Figure 20). The frequency distribution by weight is essentially continuous up to the 95th percentile (0.03 mg) and degrades thereafter (Figure 21a). On a standard log-log plot of mesh size vs. number of MD/tonne, the size distribution curve is linear and steep (Figure 21b), suggesting that macrodiamonds (>0.5 mm in the two largest dimensions) may be present in the sampled bed, but are likely rare.

Discussion and recommendations for future study

The lapilli tuff of sample LX/KL-3 is interpreted to represent pyroclastic material deposited by primary volcaniclastic processes and may therefore more closely reflect the composition of its source magma as compared to the polymictic conglomerate of sample LX/KL-2. The major and trace element geochemistry and alkaline affinity of the lapilli tuff, and its chemical similarity to 'Type 1' lamprophyre dikes at Oxford Lake and Knee Lake, indicate that it likely derives from lamprophyric volcanism. Notably, the association of chromite, Cr-spinel and Cr-diopside in the lapilli tuff is comparable to the HP diatreme in British Columbia, which is likewise composed of alkaline lamprophyre, and is non-diamondiferous (Fipke et al., 1995). Although the compositions of spinel in these rocks are different, most are inconsistent with kimberlitic sources, as is the absence of garnet and ilmenite – common indicator minerals for kimberlite. Nevertheless, the lapilli tuff contains diamond-inclusion Cr-spinel, as well as Cr-diopside that plots within the compositional field for Cr-diopside included in diamond,

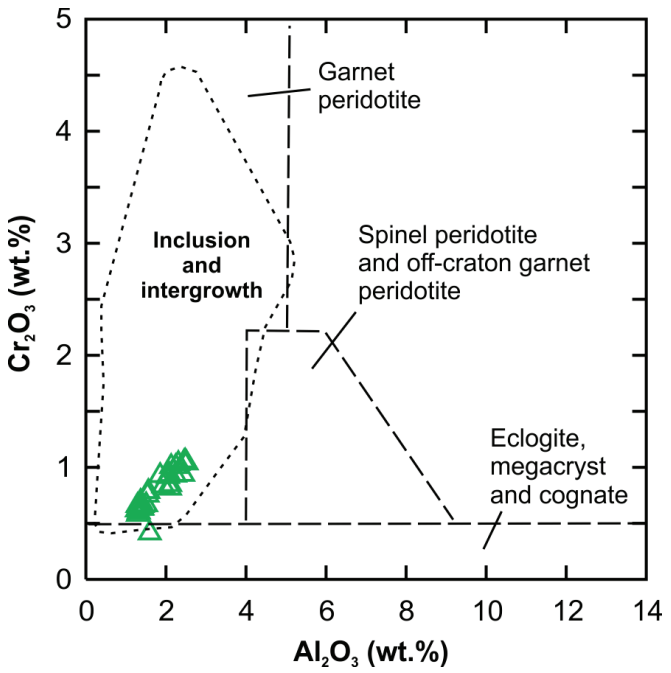

Figure 19: *Bivariate plot (Al_2O_3 vs. Cr_2O_3) of compositional data for Cr-diopside grains from sample KL-3; compositional field for diamond-inclusion and diamond-intergrowth Cr-diopside is from Nimis (2002); other compositional fields are from Ramsay and Tompkins (1994).*

Table 3: Microdiamond data for sample LX-2.

Sieve size (mm)	Diamonds (#)	Total weight (mg)	Total weight (ct)	Mean weight (mg)	Mean diamond size (ct)	Diamonds per tonne
0.425	1	0.2071	0.00104	0.2071	0.00104	63
0.300	4	0.3196	0.00160	0.0799	0.00040	253
0.212	8	0.2357	0.00118	0.0295	0.00015	506
0.150	25	0.3434	0.00172	0.0137	0.00007	1582
0.106	45	0.2298	0.00115	0.0051	0.00003	2848
0.075	61	0.1020	0.00051	0.0017	0.00001	3861

Figure 20: *Microdiamond (0.2071 mg) recovered from sample LX-2.*

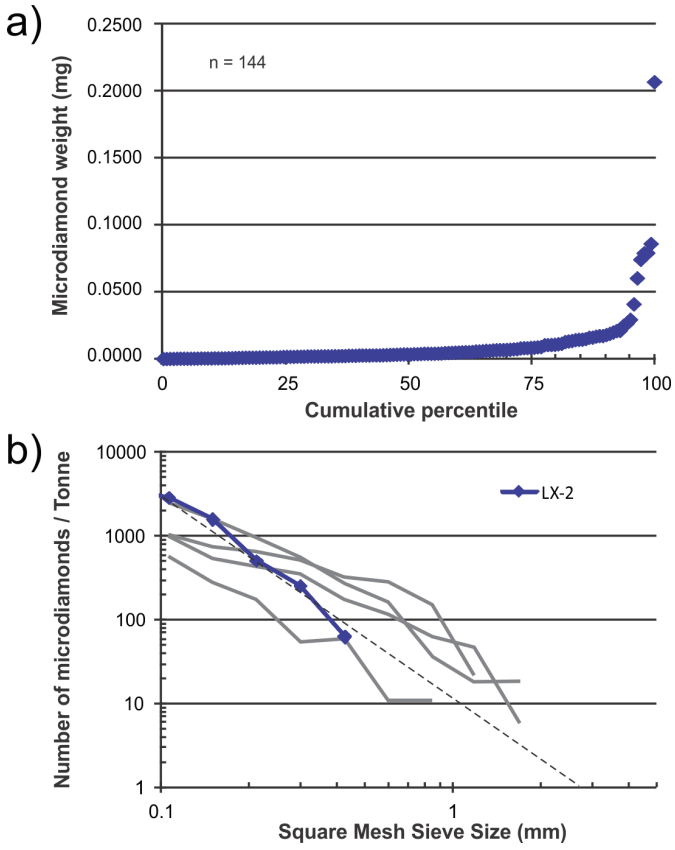

Figure 21: *Distribution plots for microdiamonds from sample LX-2:* ***a)*** *cumulative percentile plot of microdiamond size by weight, showing a continuous distribution up to the 95th percentile;* ***b)*** *square-mesh sieve size vs. number of microdiamonds/tonne (log-log) showing a linear, relatively steep distribution curve (heavy blue line; dashed line indicates best-fit); shown for comparison purposes are microdiamond distribution curves (grey lines) for samples of resedimented volcaniclastic kimberlite from the Misery complex of the Ekati mine (Krebs et al., 2016); sample LX-2 shows high concentrations of microdiamonds in the smaller size fractions, whereas the steep slope of the best-fit line suggests that the sampled bed is unlikely to contain stones larger than 2 mm.*

indicating that the source magma may have been derived from within the diamond stability field in the upper mantle (>140 km depth). Whole-rock trace element data, coupled with major-element data from the indicator minerals, point to a metasomatised mantle source. Resolving the potentially complex petrogenesis of these rocks will require additional study, with emphasis on documenting the microdiamond and indicator mineral contents and mineral chemistry of the lamprophyre dikes in comparison to the primary volcaniclastic deposits of the UFA at southern Knee Lake, as well as detailed isotopic work (C, O, Sr, Nd) to better understand potential sources.

The polymictic conglomerate of sample LX/KL-2 has markedly different field characteristics as compared to the lapilli tuff (sample LX/KL-3), indicating final deposition via normal sedimentary processes (i.e., debris flows, grain flows and low-density turbidity currents) in an alluvial or shallow-marine fan setting. The conglomerate contains diverse volcanic and plutonic clasts of ultramafic–mafic composition that were likely sourced from local basement (i.e., HRG); such clasts were not observed in sample LX/KL-3. Despite these differences, sandstone interstratified with the conglomerate is geochemically similar in most respects to the lapilli tuff, suggesting that the sedimentary deposits contain a major component of detritus derived from a similar (i.e., lamprophyric) volcanic source. This inference may be supported by the presence of pelletal lapilli in the conglomerate, which are interpreted to represent primary volcaniclastic particles related to diatreme volcanism. Indicator mineral populations and microdiamond contents of these samples are also markedly different, yet the compositional ranges and trends defined by their spinel populations are very similar, mostly overlapping the field for komatiitic

volcanic rocks. These features may result from heterogeneities in the upper mantle or different phases of lamprophyric volcanism, or could be explained by post-eruptive processes, with concentration of microdiamonds, destruction of Cr-diopside and incorporation of diverse clast types due to sedimentary reworking in the case of the conglomerate. In this regard, it is important to consider that the size distribution and abundance of microdiamonds in the conglomerate was likely modified by washing in the subaerial to shallow marine depositional setting.

Future work to differentiate between these or other possibilities should focus on documenting the sedimentology of these unusual deposits in detail, and determining the microdiamond and/or indicator mineral contents and mineral chemistry in comparison to other conglomerate beds, volcaniclastic deposits, and various compositional types of lamprophyre dikes at Knee Lake and Oxford Lake. Any macrodiamonds recovered from these rocks could be further characterized on the basis of morphology, colour, mineral inclusions, cathodoluminescence and nitrogen systematics for the purpose of establishing the origin and paragenesis of the diamonds, and understanding their provenance in comparison to any other diamondiferous rocks in the region.

Economic considerations

This report documents the newly discovered microdiamond occurrence at southern Knee Lake, and sheds light on the nature, distribution, structure and geochemistry of the unusual hostrocks, with implications for diamond exploration. The southern Knee Lake occurrence represents the first discovery of diamonds associated with alkaline volcanic rocks in Manitoba, and is the second such discovery in rocks of Archean age in the Superior province, the first being the 'unconventional' diamondiferous rocks in the Michipicoten greenstone belt of the Wawa-Abitibi terrane (south-central Superior province) near Wawa, Ontario.

The widespread occurrence of mantle-derived indicator minerals, commonly referred to as 'kimberlite indicator minerals' due to their usefulness in locating kimberlite pipes (the principal worldwide hostrock of conventional diamond deposits), has been recognized in surficial sediments in the Knee Lake area for close to 20 years (Fedikow et al., 2000). However, a bedrock source of these minerals, some of which are indicative of diamondiferous hostrocks (Fedikow et al., 2002a; Trommelen, 2015), had not been identified despite a surge in diamond exploration between 1999 and 2004 (Syme et al., 2004). Although diamonds are typically hosted by kimberlite intrusions (e.g., Kjarsgaard, 2007), significant deposits and occurrences are also associated with other types of mantle-derived intrusions, including lamproite and ultramafic lamprophyre, and calcalkaline lamprophyre (e.g., Gurney et al., 2005). Examples of the latter association in the Michipicoten belt near Wawa, Ontario, are strongly analogous to the Knee Lake diamond occurrence and have been the subject of a considerable number of investigations, providing insight into the potential complexity of these systems, with relevance to exploration methodologies, as summarized briefly below.

Unconventional diamond occurrences in the Wawa region are hosted by calcalkaline lamprophyre intrusions and polymict volcaniclastic breccias of lamprophyric affinity (Sage, 2000; Stone and Semenyna, 2004; Lefebvre et al., 2005), and alluvial and submarine-fan conglomerates (Bruce, 2011). Mutual crosscutting relationships of diamondiferous dikes and breccia are interpreted to reflect episodic lamprophyric magmatism (Lefebvre et al., 2005). U-Pb geochronology indicates broadly coeval lamprophyric volcanism (ca. 2.7–2.67 Ga; Ayer et al., 2003; Stone and Semenyna, 2004; Vaillancourt et al., 2004) and sedimentation (ca. 2.7 Ga; Bruce et al., 2010; Bruce, 2011), although structural complexities and poor exposure preclude unequivocal correlation of diamondiferous units. The dikes and breccia do not contain kimberlitic indicator minerals (Sage, 2000; Stone and Semenyna, 2004), whereas the conglomerate contains picroilmenite with compositions typical of kimberlite (Kopylova et al., 2011), suggesting different sources; studies of diamonds in these rocks also support distinct origins (Bruce et al., 2010; Bruce, 2011). Mineral inclusion data indicate that the breccia diamonds were sourced from depleted lithospheric mantle (Stachel et al., 2006), which may have included a component of subducted oceanic crust (De Stefano et al., 2006). Kimberlitic indicator minerals in the conglomerate are thought to provide indirect evidence for Archean kimberlite (Kopylova et al., 2011). However, the only known kimberlites in the region are much younger (Kaminsky et al., 2002; Heaman et al., 2004), in keeping with other Archean cratons where the vast majority of kimberlites are Mesoproterozoic (ca. 1200 Ma) or younger (Heaman et al., 2004; Gurney et al., 2010). The region also contains Mesoproterozoic dikes of ultramafic lamprophyre (Queen et al., 1996; Heaman et al., 2004), indicating that both lamprophyric and kimberlitic magmatism of at least two different ages occurred in the region.

A similarly complex scenario may well exist in the Knee Lake area, where primitive alkaline volcaniclastic deposits and associated volcanic conglomerate of Archean age are possible analogues of the Wawa diamondiferous rocks. New mapping by Anderson et al. (2015a) indicates that occurrences of the UFA are widespread at southern Knee Lake and extend inland along strike to both the northwest and southeast. However, as is the case in the Michipicoten belt, poor exposure and complex structure preclude stratigraphic correlations. Field relationships suggest that lamprophyric volcanism at southern Knee Lake may have been protracted, occurring both before and after development of synorogenic sedimentary basins. Kimberlitic indicator minerals, including peridotitic G9 and G10 garnet, Mg-ilmenite and high-Mg spinel (>10 wt. % MgO), are widespread in surficial sediments (Fedikow et al., 2002a; Trommelen, 2015) and are also found in Archean polymictic conglomerate at northern Knee Lake (sample LX/KL-1), providing indirect evidence of kimberlitic volcanism in the region, some of which may have occurred in the Archean. In contrast, the lamprophyric rocks lack garnet and ilmenite, and contain mostly low-Mg spinel, suggesting that they were not a significant source of the indicator minerals recovered from surficial sediments in the Knee Lake region (i.e., the kimberlitic indicator minerals were derived from different sources, yet to be identified). At southern Knee Lake, drift prospecting is further complicated by a number of factors, including several directions of ice flow (as indicated by field-based ice-flow indicators), widespread dilution of the local bedrock signature by far-travelled calcareous

till, streamlined landforms that do not reflect the ice-flow transport direction, and a locally thick blanket of glaciolacustrine clay (Trommelen, 2015).

For these reasons, the initial stages of follow-up exploration should focus on detailed mapping of lamprophyric volcaniclastic, sedimentary and intrusive rocks, and the collection of well-constrained bedrock samples for caustic fusion and heavy mineral separation in order to establish the spatial distribution of diamondiferous rocks and the nature of their indicator mineral populations. In addition, an orientation survey of surficial sediments inland from the eastern and western bays, including detailed characterization of the glacial till as per the recommendations of Trommelen (2015), as well as conventional geochemical analysis for elements known to be enriched in the diamondiferous rocks (e.g., Ba, Cr, Ni, Sr), may also prove valuable. More regionally, lamprophyre intrusions up to 40 m thick in the west-central portion of Gods Lake (Gilbert, 1985) may represent compelling exploration targets, as they are situated on the opposite (southeast) side of the Bayly Lake pluton from the occurrences at Knee Lake and are not known to have been assessed for diamonds. New lake-sediment geochemical data for the region (McCurdy et al., 2016) may also provide a practical tool for identifying areas of enhanced potential for primitive alkaline volcanic rocks.

Acknowledgments

J. Deyholos, D. Downie and M. Stocking (University of Manitoba) provided capable and enthusiastic assistance during the field mapping component of this study. The author benefited from discussions with R. Syme, T. Corkery and A. Chakhmouradian, and C. Böhm provided a thorough review of the manuscript. Mineral separation and analysis (microdiamonds and indicator minerals) was funded by Mount Morgan Resources Ltd. (M. Fedikow), Polaris Capital Ltd. (R. Day), Indicator Explorations Ltd. (J. Lee) and H. Westdal.

References

Anderson, S.D., Kremer, P.D. and Martins, T. 2012a: Geology and structure of southwest Oxford Lake (east part), Manitoba (parts of NTS 53L12, 13); Manitoba Innovation, Energy and Mines, Manitoba Geological Survey, Preliminary Map PMAP2012-2, 1:20 000 scale.

Anderson, S.D., Kremer, P.D. and Martins, T. 2012b: Geology and structure of southwest Oxford Lake (west part), Manitoba (parts of NTS 53L12, 13, 63I9, 16); Manitoba Innovation, Energy and Mines, Manitoba Geological Survey, Preliminary Map PMAP2012-1, 1:20 000 scale.

Anderson, S.D., Kremer, P.D. and Martins, T. 2012c: Preliminary results of bedrock mapping at Oxford Lake, northwestern Superior Province, Manitoba (parts of NTS 53L12, 13, 63I9, 16); *in* Report of Activities 2012, Manitoba Innovation, Energy and Mines, Manitoba Geological Survey, p. 6–22.

Anderson, S.D., Kremer, P.D. and Martins, T. 2013a: Geology and structure of northeastern Oxford Lake, Manitoba (parts of NTS 53L13, 14): sheet 1; Manitoba Mineral Resources, Manitoba Geological Survey, Preliminary Map PMAP2013-1, 1:20 000 scale.

Anderson, S.D., Kremer, P.D. and Martins, T. 2013b: Geology and structure of northeastern Oxford Lake, Manitoba (parts of NTS 53L13, 14): sheet 2; Manitoba Mineral Resources, Manitoba Geological Survey, Preliminary Map PMAP2013-2, 1:20 000 scale.

Anderson, S.D., Kremer, P.D. and Martins, T. 2013c: Geology and structure of northeastern Oxford Lake, Manitoba (parts of NTS 53L13, 14): sheet 3; Manitoba Mineral Resources, Manitoba Geological Survey, Preliminary Map PMAP2013-3, 1:20 000 scale.

Anderson, S.D., Kremer, P.D. and Martins, T. 2013d: Preliminary results of bedrock mapping at Oxford Lake, northwestern Superior province, Manitoba (parts of NTS 53L13, 14); *in* Report of Activities 2013, Manitoba Mineral Resources, Manitoba Geological Survey, p. 7–22.

Anderson, S.D., Syme, E.C., Corkery, M.T., Bailes, A.H. and Lin, S. 2015a: Bedrock geology of the southern Knee Lake area, Manitoba (parts of NTS 53L14, 15); Manitoba Mineral Resources, Manitoba Geological Survey, Preliminary Map PMAP2015-1, 1:20 000 scale.

Anderson, S.D., Syme, E.C., Corkery, M.T., Bailes, A.H. and Lin, S. 2015b: Preliminary results of bedrock mapping at southern Knee Lake, northwestern Superior province, Manitoba (parts of NTS 53L14, 15); *in* Report of Activities 2015, Manitoba Mineral Resources, Manitoba Geological Survey, p. 9–23.

Anderson, S.D. 2016a: Alkaline rocks at Oxford Lake and Knee Lake, northwestern Superior province, Manitoba (NTS 53L13, 14, 15): preliminary results of new bedrock mapping and lithogeochemistry; *in* Report of Activities 2016, Manitoba Growth, Enterprise and Trade, Manitoba Geological Survey, p. 16–27.

Anderson, S.D. 2016b: Preliminary results of bedrock mapping at central Knee Lake, northwestern Superior province, Manitoba (parts of NTS 53L15, 53M2); *in* Report of Activities 2016, Manitoba Growth, Enterprise and Trade, Manitoba Geological Survey, p. 1–15.

Anderson, S.D., Syme, E.C. and Corkery, M.T. 2016: Bedrock geology of south-central Knee Lake, Manitoba (parts of NTS 53L15, 53M2); Manitoba Growth, Enterprise and Trade, Manitoba Geological Survey, Preliminary Map PMAP2016-1, 1:15 000 scale.

Ayer, J.A., Conceição, R.V., Ketchum, J.W.F., Sage, R.P., Semenyna, L. And Wyman, D.A. 2003: The timing and petrogenesis of diamondiferous lamprophyres in the Michipicoten and Abitibi greenstone belts; *in* Summary of Field Work and Other Activities 2003, Ontario Geological Survey, Open File Report 6120, p. 10-1–10-9.

Barnes, S.J. and Roeder, P.L. 2001: The range of spinel compositions in terrestrial mafic and ultramafic rocks; Journal of Petrology, v. 42, p. 2279–2302.

Barry, G.S. 1959: Geology of the Oxford House–Knee Lake area, Oxford Lake and Gods Lake Mining Divisions, 53L/14 and 53L/15; Manitoba Department of Mines and Natural Resources, Mines Branch, Publication 58-3, 39 p.

Barry, G.S. 1960: Geology of the western Oxford Lake–Carghill Island area, Oxford Lake Mining Division, 53L/13; Manitoba Department of Mines and Natural Resources, Mines Branch, Publication 59-2, 37 p.

Barry, G.S. 1964: Geology of the Parker Lake area, 53M/2, Gods Lake Mining Division, Manitoba; Manitoba Department of Mines and Natural Resources, Mines Branch, Publication 62-1, 26 p.

Bell, R. 1879: Report on the country between Lake Winnipeg and Hudson Bay; Geological and Natural History Survey of Canada, Report of Progress for 1877–78, Part CC.

Bell, R. 1881: Report on Hudson's Bay and some of the lakes and rivers lying to the west of it; Geological and Natural History Survey of Canada, Report of Progress for 1879–80, Part C, p. 1C–113C.

Brock, R.W. 1911: The Hudson Bay route; *in* Summary Report of the Geological Survey Branch of the Department of Mines for the calendar year 1910; Sessional Paper 26, p. 14–26.

Brooks, C., Ludden, J., Pigeon, Y. and Hubregtse, J.J.M.W. 1982: Volcanism of shoshonite to high-K andesite affinity in an Archean arc environment, Oxford Lake, Manitoba; Canadian Journal of Earth Sciences, v. 19, p. 55–67.

Bruce, E.L. 1920: Knee Lake district, northeastern Manitoba; Canada Department of Mines, Geological Survey, Summary Report, 1919, Part D, p. 1D–11D.

Bruce, L.F. 2011: Diamonds in an Archean greenstone belt: a study of diamonds and host meta-conglomerate from Wawa (northern Ontario); M.Sc. thesis, University of British Columbia, Vancouver, 249 p.

Bruce, L.F., Kopylova, M.G., Longo, M. and Ryder, J. 2010: Diamonds in an Archean greenstone belt: diamond suites in unconventional rocks of Wawa, northern Ontario (Canada); GeoCanada 2010 conference, Calgary, Alberta, May 10–14, 2010 (extended abstract).

Cabanis, B. and Lecolle, M. 1989: Le diagramme La/10-Y/15-Nb/8: un outil pour la discrimination des series volcaniques et la mise en evidence des processus de mélange et/ou de contamination crustale; Comptes Rendus de l'Academie des Sciences, v. 309, p. 2023–2029.

Chakhmouradian, A.R., Böhm, C.O., Kressall, R.D. and Lenton, P.G. 2008: Evaluation of the age, extent and composition of the Cinder Lake alkaline intrusive complex, Knee Lake area, Manitoba (part of NTS 53L15); *in* Report of Activities 2008, Manitoba Science, Technology, Energy and Mines, Manitoba Geological Survey, p. 109–120.

Corkery, M.T., Cameron, H.D.M., Lin, S., Skulski, T., Whalen, J.B. and Stern, R.A. 2000: Geological investigations in the Knee Lake belt (parts of NTS 53L); *in* Report of Activities 2000, Manitoba Industry, Trade and Mines, Manitoba Geological Survey, p. 129–136.

De Stefano, A., Lefebvre, N. and Kopylova, M. 2006: Enigmatic diamonds in Archean calc-alkaline lamprophyres of Wawa, southern Ontario, Canada; Contributions to Mineralogy and Petrology, v. 151, p. 158–173.

Donak, T.B. 2016: Carbonate dikes at Knee Lake, Oxford Lake–Knee Lake greenstone belt, northwestern Superior Province, Manitoba; B.Sc. technical report, University of Manitoba, Winnipeg, 47 p.

Fedikow, M.A.F., Nielsen, E., Conley, G.G. and Lenton, P.G. 2000: Operation Superior: multimedia geochemical and mineralogical survey results from the southern portion of the Knee Lake greenstone belt, northern Superior Province, Manitoba (NTS 53L); Manitoba Industry, Trade and Mines, Geological Survey, Open File Report OF2000-2.

Fedikow, M.A.F., Nielsen, E., Conley, G.G. and Lenton, P.G. 2001: Operation Superior: kimberlite indicator mineral survey results (2000) for the northern half of the Knee Lake greenstone belt, northern Superior Province, Manitoba (NTS 53M/1, 2, 3, 7 and 53L/15); Manitoba Industry, Trade and Mines, Manitoba Geological Survey, Open File Report OF2001-5.

Fedikow, M.A.F., Nielsen, E., Conley, G.G. and Lenton, P.G. 2002a: Operation Superior: compilation of kimberlite indicator mineral survey results (1996–2001); Manitoba Industry, Trade and Mines, Manitoba Geological Survey, Open File Report OF2002-1.

Fedikow, M.A.F., Nielsen, E., Conley, G.G. and Lenton, P.G. 2002b: Operation Superior: multimedia geochemical survey results from the northern portion of the Knee Lake greenstone belt, northern Superior Province, Manitoba (NTS 53L); Manitoba Industry, Trade and Mines, Manitoba Geological Survey, Open File Report OF2001-1.

Fipke, C.E., Gurney, J.J. and Moore, R.O. 1995: Diamond exploration techniques emphasising indicator mineral geochemistry and Canadian examples; Geological Survey of Canada, Bulletin 423, 86 p.

Gernon, T.M., Brown, R.J., Tait, M.A. and Hincks, T.K. 2012: The origin of pelletal lapilli in explosive kimberlite eruptions; Nature Communications, v. 3, art. 832, 7 p.

Gilbert, H.P. 1985: Geology of the Knee Lake–Gods Lake area; Manitoba Energy and Mines, Geological Services, Geological Report GR83-1B, 76 p.

Grütter, H.S., Gurney, J.J., Menzies, A.H. and Winter, F. 2004: An updated classification scheme for mantle-derived garnet, for use by diamond explorers; Lithos, v. 77, p. 841–857.

Gurney, J.J., Helmstaedt, H.H., Le Roex, A.P., Nowicki, T.E., Richardson, S.H. and Westerlund, K.J. 2005: Diamonds: crustal distribution and formation processes in time and space and an integrated deposit model; Economic Geology 100th Anniversary Volume, p. 143–177.

Gurney, J.J., Helmstaedt, H.H., Richardson, S.H. and Shirey, S.B. 2010: Diamonds through time; Economic Geology, v. 105, p. 689–712.

Heaman, L.M., Kjarsgaard, B.A. and Creaser, R.A. 2004: The temporal evolution of North American kimberlites; Lithos, v. 76, p. 377–397.

Hubregtse, J.J.M.W. 1978: Chemistry of cyclic subalkaline and younger shoshonitic volcanism in the Knee Lake–Oxford Lake greenstone belt, northeastern Manitoba; Manitoba Department of Mines, Resources and Environmental Management, Mineral Resources Division, Geological Paper 78/2, 18 p.

Hubregtse, J.J.M.W. 1985: Geology of the Oxford Lake–Carrot River area; Manitoba Energy and Mines, Geological Services, Geological Report GR83-1A, 73 p.

Kamenetsky, V.S., Crawford, A.J. and Meffre, S. 2001: Factors controlling chemistry of magmatic spinel: an empirical study of associated olivine, Cr-spinel and melt inclusions from primitive rocks; Journal of Petrology, v. 42, p. 655–671.

Kaminsky, F.V., Sablukov, S.M., Sablukova, L.I., Shchukin, V.S. and Canil, D. 2002: Kimberlites from the Wawa area, Ontario; Canadian Journal of Earth Sciences, v. 39, p. 1819–1838.

Kjarsgaard, B.A. 2007: Kimberlite diamond deposits; *in* Mineral Deposits of Canada: A Synthesis of Major Deposit Types, District Metallogeny, the Evolution of Geological Provinces, and Exploration Methods, W.D. Goodfellow (ed.), Geological Association of Canada, Mineral Deposits Division, Special Publication No. 5, p. 245–272.

Kopylova, M.G., Afanasiev, V.P., Bruce, L.F., Thurston, P.C. and Ryder, J. 2011: Metaconglomerate preserves evidence for kimberlite, diamondiferous root and medium grade terrane of a pre-2.7 Ga Southern Superior protocraton; Earth and Planetary Science Letters, v. 312, p. 213–225.

Krebs, M.Y., Pearson, D.G., Stachel, T., Stern, R.A., Nowicki, T. and Cairns, S. 2016: Using microdiamonds in kimberlite diamond grade prediction: a case study of the variability in diamond population characteristics across the size range 0.2 to 3.4 mm in Misery kimberlite, Ekati mine, NWT, Canada; Economic Geology, v. 111, p. 503–525.

Kressall, R.D. 2012: The petrology, mineralogy and geochemistry of the Cinder Lake alkaline intrusive complex, eastern Manitoba; M.Sc. thesis, University of Manitoba, Winnipeg, Manitoba, 396 p.

Kressall, R.D., Chakhmouradian, A.R. and Böhm, C.O. 2010: Petrological and geochemical investigation of the Cinder Lake alkaline intrusive complex, Knee Lake area, east-central Manitoba (part of NTS 53L15); *in* Report of Activities 2010, Manitoba Innovation, Energy and Mines, Manitoba Geological Survey, p. 146–158.

Lefebvre, N., Kopylova, M. and Kivi, K. 2005: Archean calc-alkaline lamprophyres of Wawa, Ontario, Canada: unconventional diamondiferous volcaniclastic rocks; Precambrian Research, v. 138, p. 57–87.

Lenton, P.G. 1985: Granite-pegmatite investigations: Knee Lake-Magill Lake area; *in* Report of Field Activities 1985, Manitoba Energy and Mines, Geological Services, p. 203–208.

Lin, S. and Jiang, D. 2001: Using along-strike variation in strain and kinematics to define the movement direction of curved transpressional shear zones: an example from northwestern Superior Province, Manitoba; Geology, v. 29, p. 767–770.

Lin, S., Jiang, D., Syme, E.C., Corkery, M.T. and Bailes, A.H. 1998: Structural study in the southern Knee Lake area, northwestern Superior Province, Manitoba (part of NTS 53L/15); *in* Report of Activities, 1998, Manitoba Energy and Mines, Geological Services, p. 96–102.

Lin, S., Davis, D.W., Rotenberg, E., Corkery, M.T. and Bailes, A.H. 2006: Geological evolution of the northwestern Superior Province: clues from geology, kinematics, and geochronology in the Gods Lake Narrows area, Oxford–Stull terrane, Manitoba; Canadian Journal of Earth Sciences, v. 43, p. 749–765.

McCurdy, M.W., Böhm, C.O., Anderson, S.D., Gauthier, M.S. and Amor, S.D. 2016: Geochemical Data for Lake Sediments in the Superior Province of Manitoba (NTS 53-E, 53-L and 53-M); Geological Survey of Canada, Open File 8179; Manitoba Geological Survey Open File OF2016-1, 23 p.

McInnes, W. 1913: The basins of Nelson and Churchill Rivers; Geological Survey of Canada, Memoir 30, 146 p.

Nimis, P. 2002: The pressures and temperatures of formation of diamond based on thermobarometry of chromian diopside inclusions; The Canadian Mineralogist, v. 40, p. 871–884.

Nowicki, T.E., Moore, R.O., Gurney, J.J. and Baumgartner, M.C. 2007: Diamonds and associated heavy minerals in kimberlite: a review of key concepts and applications; Developments in Sedimentology, v. 58, p. 1235–1267.

Pearce, J.A. 2008: Geochemical fingerprinting of oceanic basalts with applications to ophiolite classification and the search for Archean oceanic crust; Lithos, v. 100, p. 14–48.

Pearce, J.A. and Peate, D.W. 1995: Tectonic implications of the composition of volcanic arc magmas; Annual Review of Earth and Planetary Sciences, v. 23, p. 251–285.

Peccerillo, A. and Taylor, S.R. 1976: Geochemistry of Eocene calc-alkaline volcanic rocks from the Kastamonu area, northern Turkey; Contribution to Mineralogy and Petrology, v. 58, p. 63–81.

Percival, J.A., Sanborn-Barrie, M., Skulski, T., Stott, G.M., Helmstaedt, H. and White, D.J. 2006: Tectonic evolution of the western Superior Province from NATMAP and LITHOPROBE studies; Canadian Journal of Earth Sciences, v. 43, p. 1085–1117.

Queen, M., Heaman, L.M., Hanes, J.A., Archibald, D.A. and Farrar, E. 1996: $^{40}Ar/^{39}Ar$ and U–Pb perovskite dating of lamprophyre dykes from the eastern Lake Superior region: evidence for a 1.14 Ga magmatic precursor to the Midcontinent Rift volcanism; Canadian Journal of Earth Sciences, v. 33, p. 958–965.

Quinn, H.A. 1955: Knee Lake, Manitoba; Geological Survey of Canada, Paper 55-8 (map with marginal notes).

Ramsay, R.R. and Tompkins, L.A. 1994: The geology, heavy mineral concentrate mineralogy, and diamond prospectivity of the Boa Esperança and Cana Verde pipes, Corrego D'anta, Minas Gerais, Brazil; *in* Kimberlites, Related Rocks and Mantle Xenoliths, H.O.A. Meyer and O.H. Leonardos (eds.), Proceedings of the 5th International Kimberlite Conference, Araxá, Brazil, Companhia de Pesquisa de Recursos Minerais (CRPM), Special Publication, v. 2, p. 329–345.

Reimer, E.R. 2014: Petrography, mineralogy and geochemistry of carbonate rocks at Oxford Lake, Oxford Lake–Knee Lake greenstone belt, northwestern Superior Province, Manitoba; B.Sc. thesis, University of Manitoba, Winnipeg, 112 p.

Richardson, D.J., Ostry, G., Weber, W. and Fogwill, W.D. 1996: Gold deposits of Manitoba; Manitoba Energy and Mines, Economic Geology Report ER86-1 (2nd Edition), 114 p.

Roeder, P.L. and Schulze, D.J. 2008: Crystallization of groundmass spinel in kimberlite; Journal of Petrology, v. 49, p. 1473–1495.

Sage, R.P. 2000: The "Sandor" diamond occurrence, Michipicoten greenstone belt, Wawa, Ontario: a preliminary study; Ontario Geological Survey, Open File Report 6016, 49 p.

Skulski, T., Corkery, M.T., Stone, D., Whalen, J.B. and Stern, R.A. 2000: Geological and geochronological investigations in the Stull Lake–Edmund Lake greenstone belt and granitoid rocks of the northwestern Superior Province; *in* Report of Activities 2000, Manitoba Industry, Trade and Mines, Manitoba Geological Survey, p. 117–128.

Southard, G.G. 1977: Exploration history, compilation and review, including exploration data from cancelled assessment files, for the Gods, Knee and Oxford lakes areas, Manitoba; Manitoba Department of Mines, Resources and Environmental Management, Mineral Resources Division, Open File Report 77/5, 93 p.

Stachel, T., Banas, A., Muehlenbachs, K., Kurszlaukis, S. and Walker, E.C. 2006: Archean diamonds from Wawa (Canada): samples from deep cratonic roots predating cratonization of the Superior Province; Contributions to Mineralogy and Petrology, v. 151, p. 737–750.

Stone, D. and Semenyna, L. 2004: Petrography, chemistry and diamond characteristics of heterolithic breccia and lamprophyre dikes at Wawa, Ontario; Ontario Geological Survey, Open File Report 6134, 39 p.

Stott, G.M., Corkery, M.T., Percival, J.A., Simard, M. and Goutier, J. 2010: A revised terrane subdivision of the Superior Province; *in* Summary of Field Work and Other Activities 2010, Ontario Geological Survey, Open File Report 6260, p. 20-1–20-10.

Sun, S-s. and McDonough, W.F. 1989: Chemical and isotopic systematics of oceanic basalts: implications for mantle composition and processes; *in* Magmatism in the Ocean Basins, A.D. Saunders and M.J. Norry (ed.), Geological Society of London, Special Publications, v. 42, p. 313–345.

Syme, E.C., Corkery, M.T., Bailes, A.H., Lin, S., Cameron, H.D.M. and Prouse, D. 1997: Geological investigations in the Knee Lake area, northwestern Superior Province (parts of NTS 53L/15 and 53L/14); *in* Report of Activities, 1997, Manitoba Energy and Mines, Geological Services, p. 37–46.

Syme, E.C., Corkery, M.T., Lin, S., Skulski, T. and Jiang, D. 1998: Geological investigations in the Knee Lake area, northern Superior Province (parts of NTS 53L/15 and 53M/2); *in* Report of Activities, 1998, Manitoba Energy and Mines, Geological Services, p. 88–95.

Syme, E.C., Corkery, M.T., Bailes, A.H., Lin, S., Skulski, T. and Stern, R.A. 1999: Towards a new tectonostratigraphy for the Knee Lake greenstone belt, Sachigo subprovince, Manitoba; *in* Western Superior Transect 5th Annual Workshop; R.M. Harrap and H.H. Helmstaedt (eds.); Lithoprobe Secretariat; The University of British Columbia, Vancouver, BC; Lithoprobe Report 70, p. 124–131.

Syme, E.C., Bezys, R.K., Bogdan, D.J., Böhm, C.O., Kaszycki, C.A., Keller, G.R., Lenton, P.G. and Matile, G.L.D. 2004: Kimberlite potential in Manitoba: an update; *in* Report of Activities 2004, Manitoba Industry, Economic Development and Mines, Manitoba Geological Survey, p. 309–319.

Trommelen, M.S. 2014a: Surficial geology of the Knee Lake map area, Manitoba (NTS 53L15); Manitoba Mineral Resources, Manitoba Geological Survey, Geoscientific Map MAP2013-9, scale 1:50 000.

Trommelen, M.S. 2014b: Surficial geology of the Makakaysip Lake area, Manitoba (NTS 53M1); Manitoba Mineral Resources, Manitoba Geological Survey, Geoscientific Map MAP2013-6, scale 1:50 000.

Trommelen, M.S. 2014c: Surficial geology of the Mines Point map area, Manitoba (NTS 53M2); Manitoba Mineral Resources, Manitoba Geological Survey, Geoscientific Map MAP2013-7, scale 1:50 000.

Trommelen, M.S. 2014d: Surficial geology of the Oxford House map area, Manitoba (NTS 53L14); Manitoba Mineral Resources, Manitoba Geological Survey, Geoscientific Map MAP2013-8, scale 1:50 000.

Trommelen, M.S. 2015: Glacial history and till composition, Knee Lake area, northeastern Manitoba (NTS 53L14, 15, 53M1, 2); Manitoba Mineral Resources, Manitoba Geological Survey, Geoscientific Paper GP2013-3, 30 p. plus 13 appendices.

Vaillancourt, C., Ayer, J.A., Zubowski, S.M. and Kamo, S.L. 2004: Synthesis and timing of Archean geology and diamond-bearing rocks in the Michipicoten greenstone belt: Menzies and Musquash Townships; *in* Summary of Field Work and Other Activities 2004, Ontario Geological Survey, Open File Report 6145, p. 6-1–6-9.

Wright, J.F. 1926: Oxford and Knee Lakes area, northern Manitoba; *in* Canada Department of Mines, Geological Survey, Summary Report, 1925, Part B, p. 16B–26B.

Wright, J.F. 1932: Oxford House area, Manitoba; *in* Canada Department of Mines, Geological Survey, Summary Report, 1931, Part C, p. 1C–25C.